Graduate School ETD Form 9
(Revised 12/07)

PURDUE UNIVERSITY
GRADUATE SCHOOL
Thesis/Dissertation Acceptance

This is to certify that the thesis/dissertation prepared

By Lindsay Jo Hammack

Entitled
Identification of the Pba1 and Pba2 Binding Sites on 20S Core Particle Intermediates

For the degree of Master of Science

Is approved by the final examining committee:

Andrew Kusmierczyk
Chair

Stephen Randall

Anna Malkova

To the best of my knowledge and as understood by the student in the *Research Integrity and Copyright Disclaimer (Graduate School Form 20)*, this thesis/dissertation adheres to the provisions of Purdue University's "Policy on Integrity in Research" and the use of copyrighted material.

Approved by Major Professor(s): Andrew Kusmierczyk

Approved by: Simon Atkinson 07/09/2012
Head of the Graduate Program Date

Graduate School Form 20
(Revised 9/10)

PURDUE UNIVERSITY
GRADUATE SCHOOL

Research Integrity and Copyright Disclaimer

Title of Thesis/Dissertation:

Identification of the Pba1 and Pba2 Binding Sites on 20S Core Particle Intermediates

For the degree of Master of Science

I certify that in the preparation of this thesis, I have observed the provisions of *Purdue University Executive Memorandum No. C-22,* September 6, 1991, *Policy on Integrity in Research.**

Further, I certify that this work is free of plagiarism and all materials appearing in this thesis/dissertation have been properly quoted and attributed.

I certify that all copyrighted material incorporated into this thesis/dissertation is in compliance with the United States' copyright law and that I have received written permission from the copyright owners for my use of their work, which is beyond the scope of the law. I agree to indemnify and save harmless Purdue University from any and all claims that may be asserted or that may arise from any copyright violation.

Lindsay Jo Hammack

Printed Name and Signature of Candidate

07-09-2012

Date (month/day/year)

*Located at http://www.purdue.edu/policies/pages/teach_res_outreach/c_22.html

IDENTIFICATION OF THE PBA1 AND PBA2 BINDING SITES ON 20S CORE PARTICLE INTERMEDIATES

A Thesis

Submitted to the Faculty

of

Purdue University

by

Lindsay Jo Hammack

In Partial Fulfillment of the

Requirements for the Degree

of

Master of Science

August 2012

Purdue University

Indianapolis, Indiana

ACKNOWLEDGEMENTS

First and fore most, I would like to thank Dr. Andrew Kusmierczyk for his expertise, time, support, and patience throughout the course of this work. I would also like to thank my committee members, Dr. Anna Malkova and Dr. Stephen Randall for their advice and time. Additionally, I would like to thank the members of the Kusmierczyk laboratory for their support over the past two years.

TABLE OF CONTENTS

Page

LIST OF TABLES

LIST OF FIGURES

ABSTRACT

Hammack, Lindsay Jo. M.S., Purdue University, August 2012. Identification of the Pba1 and Pba2 Binding Sites on 20S Core Particle Intermediates. Major Professor: Andrew Kusmierczyk.

The proteasome is responsible for breaking down the majority of the proteins in the cell. However, a complete understanding of how this large multi-subunit protease is assembled is currently lacking. Proper and timely assembly of the proteasome is critical for the functioning of the ubiquitin-proteasome pathway, defects in which have been associated with several different cancers. A recently discovered heterodimeric proteasome assembly chaperone, Pba1p-Pba2p, has been suggested to prevent the assembly process from straying off path. Pba1p-Pba2p associates with proteasomal assembly intermediates via C-terminal HbYX motifs. The HbYX motif is a tri-peptide sequence containing a hydrophobic residue (Hb) followed by a tyrosine (Y), then any amino acid (X). This motif was originally identified in proteasomal activators, and shown to mediate the association of activators with the proteasome by inserting into intersubunit pockets on either end of the proteasome. There are seven unique intersubunit binding pockets, located between neighboring α subunits on the proteasome, to which a HbYX-containing protein can bind; which of these pockets Pba1p-Pba2p binds to remains elusive. I attempted to identify where Pba1p and Pba2p

bind via a crosslinking approach. Specific residues were mutagenized to cysteines on Pba1p, Pba2p, and the individual α subunits in order to generate crosslinkable species. By exposing yeast cells expressing these crosslinkable proteins to mild oxidizing conditions, I attempted to trap the Pba1p and Pba2p α intersubunit pocket interactions. In order to optimize crosslinking conditions, the assay was modified several ways. Additionally, measures were taken to increase detection of the crosslinked species via immunoblotting. Despite the efforts to improve the crosslinking and detection, I was unable to successfully detect a crosslinked species. However, crosslinking is a reasonable method to identify the Pba1p and Pba2p proteasomal binding sites, having been successfully used to identify binding sites for other HbYX-motif-containing proteins; further assay optimization should yield Pba1p and Pba2p proteasomal crosslinks.

CHAPTER 1. INTRODUCTION

1.1 Introduction

Orlowski and Wilk in the early 1980's were the first to describe a high molecular weight 'multicatalytic protease complex' (Wilk & Orlowski, 1983) which is now known to be the proteasome. Shortly after the purification of these 'multicatalytic protease complexes,' several others described the same complex in different eukaryotic cells, and with each new discovery came a new name such as 'prosome' (Schmid et al, 1984), 'ingensin' (Ishiura & Sugita, 1986), 'macropain' (McGuire & DeMartino, 1986), and '20S protease' (Hough et al, 1987). By the late 1980's, prosomes and the other protease complexes were shown to be nearly identical in terms of structure and at least similar in function. Eventually, the multicatalytic protease complex, prosomes, ingensin, macropain, and 20S protease would be referred to as the 20S proteasome (Arrigo et al, 1988).

When Rechsteiner and colleagues described the 20S protease in rabbit reticulocytes, they also characterized an additional protease. This protease was a multi-subunit ATP-dependent protease at a high molecular weight (Hough et al, 1987). This large multi-subunit protease eventually became referred to as the 26S proteasome.

Further characterization of this complex demonstrated that this protease was responsible for degrading ubiquitin tagged proteins within the cell (Eytan et al, 1989).

1.2 Proteasome-Ubiquitin Pathway

The 26S proteasome is the degradation component of the ubiquitin-proteasome pathway. This pathway is responsible for selectively degrading the majority of soluble proteins within the cell. There are other systems/organelles within the cell that perform degradative processes, such as lysosomes. However, the degradation that occurs in lysosomes, unlike the proteasome, is non-specific. Having a highly specific degradation system is advantageous in living systems that have highly regulated mechanisms such as the cell cycle, metabolism, and embryogenesis (reviewed by Hochstrasser, 1995).

One of the early steps in the degradation of a protein by the ubiquitin-proteasome pathway involves the modification of this protein via the covalent attachment of ubiquitin. A single ubiquitin protein is roughly 8 kDa, and it is usually linked to proteins via an isopeptide bond between the carboxyl-terminus of the ubiquitin and a lysine of the target protein. However, other linkages, such as the N-terminus of a protein, are also possible (Breitschopf et al, 1998). Ubiquitination is carried out by three enzymes: E1, E2, and E3 (Figure 1). E1, also known as the ubiquitin-activating enzyme, is responsible for adenylating the ubiquitin, creating a ternary intermediate complex that is then attacked by the sulfhydyl group of the enzyme, leading to the E1-ubiquitin thioester. A tranesterification reaction then occurs whereby the covalently-bound ubiquitin is transferred to a cysteine residue of an E2 enzyme (also called a ubiquitin conjugating enzyme). Either E2 alone, or E2 in combination with an E3

(ubiquitin-ligase), will then catalyze the addition of that activated ubiquitin to a substrate. Once a protein is monoubiquinated, it may go through several rounds of ubiquitination (reviewed by Hochstrasser, 1996).

Polyubiquitination occurs when the C-terminus of an incoming ubiquitin protein is attached to one of the seven lysine residues on a ubiquitin already attached to a substrate (Xu et al, 2009). Depending on which lysine residue the new ubiquitin attaches to can determine if the protein will be targeted for proteolysis or a non-proteolytic process, such as cell signaling. As for proteolysis, certain lysine linkages will target a substrate directly to the 26S proteasome for degradation, while other linkages will target a substrate to ERAD (Endoplasmic Reticulum Associated Degradation), which eventually leads to destruction by the 26S. It was determined that all lysine linkages, except those utilizing K63, can lead to proteasomeal degradation. K63 linkages have been implicated in non-proteaolytic pathways such as cell signaling and intracellular trafficking (reviewed by Welchman et al, 2005). K48 and to some extent K11 are the most relevant linkages for proteasome degradation. K48 linkages lead to 26S degradation (van Nocker & Vierstra, 1993), and K11 linkages have been implicated in ERAD (Endoplasmic Reticulum Associated Degradation) (Xu et al, 2009), which ends with destruction by the 26S proteasome. In addition to being polyubiquinated, a monoubiquinated protein may be deubiquitinated by a deubiquitinaing enzyme (DUBs), (reviewed by Hochstrasser, 1995). DUBs are also necessary to remove polyubiquitin chains prior to degradation by the proteasome.

1.3 26S Structure

The structure of the 26S proteasome consists of a 20S core particle (CP) capped on one or both ends by the 19S regulatory particle (RP) (DeMartino & Slaughter, 1999). The double-capped structure is approximately 2.59 MDa, while the single-capped CP is around 1.66 MDa (Saeki & Tanaka, 2012).

1.3.1 20S Structure

In eukaryotes, the 20S CP is made up of 14 different subunits, which are encoded by 14 different genes (Chen & Hochstrasser, 1995). These genes encode seven distinct α and β subunits. The α and β subunits assemble into four stacked hetero-heptameric rings: $\alpha_{(1-7)}\beta_{(1-7)}\beta_{(1-7)}\alpha_{(1-7)}$. Three of the seven β subunits (β_1, β_2, and β_5) contain propeptides that are cleaved upon 20S CP assembly, exposing a catalytically active threonine residue (Thr1) (Groll et al, 1997). The rings form a barrel-like structure that has an approximate molecular mass of 730 kDa. The central chamber of this structure is where the catalytically active threonine residues are exposed. This chamber is gated on both ends of the 20S CP by the α subunit N-terminal tails, which can be opened by activator proteins, such as the 19S RP (Groll et al, 1997).

1.3.2 19S Structure

The RP (also known as PA700) is made up of about 20 subunits with a molecular mass of 930 kDa. The RP is comprised of two types of subunits, Rpt (Regulatory Particle AAA-ATPase) and Rpn (Regulatory Particle Non-ATPase) subunits. These subunits

assemble into two major sub-complexes: a base and a lid. The base is composed of a hexameric ring of Rpt subunits and three Rpn subunits, and the lid is composed of nine Rpn subunits (Glickman et al, 1998).

Historically, the hexameric Rpt ring in the base was thought to be a flat ring where the C-termini of the Rpts inserted into the intersubunit pockets of the 20S α-ring (see below). Recent work has demonstrated that the C-termini do in fact bind to the α-ring intersubunit pockets asymmetrically (Tian et al, 2011). Moreover, the lid was thought to be associated exclusively with the base component. Lander et al (2012), Lasker et al (2012), and DeFonesca et al (2012) have all recently published new electron microscopy findings that suggest the 19S subunits are not exactly arranged as previously thought. These results have shown that the lid interacts with the base as well at the 20 CP, and the Rpt subunits are not arranged in a flat ring but in a spiral staircase (Lander et al, 2012). These new images of the 19S and the 26S are changing the way the field views the 19S regulatory particle.

1.3.3 Archaeal and Eubacterial 20S Proteasomes

20S proteasomes have been identified in both eubacteria and archaea. Even though the first proteasomes were identified in eukaryotes, the prokaryotic versions have been used to more easily study the complex eukaryotic species (Volker & Lupas, 2002). The archaeal version of the 20S proteasome consists of one type of α and one type of β subunit that form four-homoheptameric rings: $\alpha_7\beta_7\beta_7\alpha_7$. The first eubacterial proteasome was identified in *Rhodococcus* sp. These bacterial proteasomes have two

different α subunits and two different β subunits that assemble into four hexameric stacked rings (Tamura et al, 1995).

1.4 20S Proteasome Assembly

The current picture of the assembly process begins with α-ring formation, with each α-ring acting as a scaffold for β subunits (Hirano et al, 2005). The β subunits are incorporated onto the α-ring in the following order: β2, β3, β4, β5, β6, β1, and β7 (Hirano et al, 2008). Subunits β1, β2, and β5 are synthesized with propeptides. During β-ring formation in yeast, at least three different proteasomal intermediates have been characterized: the 15S complex, -β7 half-mer, and the half-proteasome (Figure 2). The 15S complex contains one α-ring with β2, β3, and β4. The - β7 half-mer consists of a α-ring plus all of the β subunits, except β7, and the half-proteasome consists of one full α-ring and one full β-ring. After they are formed, the two half proteasomes will quickly dimerize, forming four stacked rings (Li et al, 2007). At this point, the propeptides are still present on the β subunits, and the structure can be referred to as the "pre-holo proteasome," or PHP. Following half-proteasome dimerization to give rise to the PHP, the propeptides on β1, β2, and β5 are cleaved, exposing a threonine residue (Thr1), leaving three distinct catalytic activities: peptidyl-glutamyl peptide hydrolyzing activity (β1), trypsin-like activity (β2), and the chymotrypsin-like activity (β5). Therefore β subunits 1, 2, and 5 are responsible for cleaving after acidic, basic, and hydrophobic residues, respectively (Heinemeyer et al, 1997). The Thr1 hydroxyl group of these

subunits is necessary for autocatalytic (i.e. self-processing of the propeptides) and proteolytic function (Heinemeyer et al, 1997). All of the 20S subunits are essential for assembly in yeast, with the exception of α3. When α3 is deleted, a second copy of α4 takes its place (Velichutina et al, 2004). These α3Δ mutant proteasomes were shown to grow better than wild-type proteasomes in the presence of heavy metals (Kusmierczyk et al, 2008).

Once the CP is fully formed, the α subunit N-terminal tails act as a gate to the catalytic chamber, which measures 13 Å across. The chamber may be opened artificially with 0.02% SDS (Smith et al, 2007); however, *in vivo* it is opened by activators from three different families: (a) the conserved Blm10/PA200 proteins found in all eukaryotes; (b) the PA28/11S protein family, with PA28αβ hetero-heptamers and the homo-heptameric PA28γ present in higher eukaryotes; and (c) complexes composed of or containing AAA+ ATPases, like the 19S regulatory particle (Schmidt et al, 2011).

1.4.1 Archaeal and Eubacterial 20S Assembly

As previously mentioned, the archaeal version of the 20S proteasome consists of one type of α and one type of β subunit. When these subunits are expressed recombinantly in *E.coli* the α and β subunits will self-assemble into fully active 20S proteasomes indistinguishable from their natively purified counterparts. If only α subunits are expressed, these subunits will self assemble into single and double heptameric rings. However, if only the β-subunit is expressed, no ring structures are

detected (Zwickl et al, 1994). Taken together, these data corroborate the currently accepted model of α rings serving as templates for β subunit assembly. However, to date, there are no studies indicating the *in vivo* assembly process for archaeal proteasomes. The assembly process could start with α/α homodimer or an α/β heterodimer (Heinemeyer et al, 2004).

Similar to the archaeal proteasomes, when eubacterial proteasomal subunits are expressed in *E.coli*, functional proteasomes will self-assemble. However, unlike the archaeal system, α-rings are not observed in *E.coli* reconstitution. Ring structures are only formed when both the α and β subunits are expressed. These subunits assemble into half-proteasomes consisting of one heptameric α-ring adjoined to a heptameric unprocessed β-ring. When two half-proteasomes dimerize, the β subunits are processed (Zuhl et al, 1997). Since α and β subunits need to be present to form ring structures, this suggests that in bacterial 20S proteasomes α-β heterodimers form first, as opposed to α rings forming and acting as a scaffold for the entry of β subunits.

1.5 Alternate Eukaryotic 20S Proteasomes

Within higher eukaryotes, at least three alternative proteasomes have been identified: the immunoproteasome, the thymoproteasome, and the testes specific proteasome.

1.5.1 Immunoproteasome

The immunoproteasome is a protease, which is responsible for processing of antigens for presentation by the major histocompatibility complex (MHC) class I molecules. In many ways it is structurally similar to the 20S CP; however, the catalytically active β1, β2, and β5 subunits are replaced with alternative catalytically active subunits LMP2 (low molecular weight protein), LMP7 (Tanaka, 1994), and MECL1 (mulitcatyltic endopeptidase complex-like) (Groettrup et al, 1997). In the presence of interferon-γ, LMP2 (also called β1i), MECL1 (β2i), and LMP7 (β5i) are induced and replace β1, β2, and β5 subunits in the 20S CP, creating new complexes. In addition to the induction of βi subunits, a special activator is also induced, the 11S, also known as PA28 (Knowlton et al, 1997). (See activators)

1.5.2 Thymoproteasome

Another alternative proteasome found within mammals is the thymoproteasome. It is very similar to the immunoproteasome in that it contains β1i and β2i; however, its replacement for the β5 subunit is not β5i (LMP7) but β5t. Thymoproteasomes are exclusively found in cortical thymic epithelium and are necessary for efficient maturation of competent CD8+T cells (Murata et al, 2007).

1.5.3 Testes-Specific Proteasome

The third alternative proteasome found within the eukaryotic kingdom is the testes specific proteasome. A study in *Drosophila melanogaster* demonstrated that around a third of the 32 proteasome subunits have a testes specific isoform (Zhong &

Belote, 2007). Zhong and colleges sought out to characterize one of the testes-specific proteasome subunits, Prosα6T. Knockout studies of this specific subunit demonstrated a problem with post-meiotic sperm cell differentiation. Therefore, testes-specific proteasome subunit Prosα6T has a functional role in normal spermatogenesis (Zhong & Belote, 2007). The function of the other testes-specific subunits is not known.

1.6 Activators

As previously mentioned, once the 20S CP has been assembled the N-termini of the a subunits act as a gate closing off the catalytic chamber. In order to allow substrates to enter the 20S CP, the gate must be opened, and *in vivo* this gate is opened by activator proteins. The conserved function of proteasomal activators is to increase the activity of the CP. Between the known eukaryotic activators, 19S, 11S (aka PA28), and Blm10, each has been shown to associate with the CP and increase peptidase activity.

1.6.1 AAA ATPase Activators

The 19S regulatory particle base is comprised of six Rpt proteins that are part of the AAA ATPase family of proteins. Archaeal PAN and the eubacterial ARC also belong to this family. Archaeal activator PAN (proteasome-activating nucleotidase) is similar to the base of the 19S regulatory particle. It is a ring structure made up of six identical AAA ATPase subunits that bind to and activate the archaeal 20S (Zwickl et al, 1999). ARC

(AAA ATPase forming Ring-shaped Complexes) consists of six identical AAA ATPase subunits that form a ring like structure which is thought to activate 20S eubacterial proteasomes (Zhang et al, 2004).

In the base of the 19S, three of the six Rpt subunits, Rpt2, Rpt3, and Rpt5, contain a C-terminal HbYX motif (Smith et al, 2007). The HbYX motif is a tri-peptide sequence that contains a hydrophobic residue (Hb) followed by a tyrosine (Y) plus one additional residue (X). When binding to the α-ring, the carboxylate of the X residue forms a salt bridge with a lysine residue (K66 in *Thermoplasma acidophilum*) that is conserved in six of the seven α intersubunit pockets (Smith et al, 2007). These HbYX motifs are important for 19S binding and are responsible for inducing 20S CP gate opening (Rabl et al, 2008). Recently, the pockets to which each Rpt C-terminal tail binds to were mapped out via crosslinking assays (Tian et al, 2011). Certain Rpt tails occupy fixed intersubunit pockets, such as Rpt2 to α4, Rpt6 to α3, and Rpt3 to α2. Other Rpt tails have a degree of flexibility when binding to the α-ring interface, Rpt1 to α6 and α5, Rpt4 to α7 or α1, and Rpt5 to α6 or α7. Given that there are six Rpt C-terminal tails and seven intersubunit pockets on the α-ring, it seems that there should be at least one unoccupied pocket on the CP. Tian et al, (2011) suggested that there are different subpopulations of proteasomes where the flexible Rpts (1, 4, and 5) may occupy different pockets on different proteasomes.

Since the initial discovery of the archaeal 20S, only one prokaryotic activator has been characterized in *Thermoplama acidophilum,* PAN (proteasome-activating

nucleotidase). PAN consists of six identical ATPases, which form a ring structure, that dock on to one or both α-rings of the 20S. These subunits all contain the same C-terminal HbYX motif that is found on three of the 19S Rpt subunits. In fact, the HbYX motif was first described, and shown to be functionally relevant, in PAN (Smith et al, 2007). Additionally, the eubacterial proteasome from *Rhodococcus* has a AAA ATPase activator named ARC. This complex also forms a six membered ring that attaches to one or both α-rings of the 20S CP; however, unlike the 19S and PAN it does not have a C-terminal HbYX motif (Wolf et al, 1998).

1.6.2 11S Activator

The 11S activator (also known as REG and PA28) exists in two forms: the heptameric complex, which consists of PA28α and PA28β subunits, or a homomeric complex consisting of PA28γ subunits (Rechsteiner & Hill, 2005). The two different 11S activators appear to have different functions. The presence of 11S activator (PA28αβ) is induced by interferon-γ and has been implicated in having a role in the formation of the immunproteasome which processes antigens for MHC class I ligand presentation (as reviewed by (Groettrup et al, 2010). The homomeric 11S (PA28γ) has been shown to bind to the 20S CP and promote the degradation of regulatory proteins (Mao et al, 2008). Although they do not contain C-terminal HbYX motifs, the C-termini of 11S activators also mediate docking (but not gating) of 20S proteasomes (Zhang et al, 1998).

1.6.3 Blm10 Activator

Ustrell et al, (2002) were the first to describe Blm10 (also known as PA200 in humans) as a proteasomal activator that was involved in DNA repair. Specifically, this group noted that Blm10 was capable of activating the proteasomal hydrolysis of peptides, but not proteins (Ustrell et al, 2002).

Since 2002, others have suggested that Blm10 is an activator. Dange et al, (2011) recently suggested that Blm10 opens the α-ring gate in the same manner as the AAA-ATPase activators, like 19S. Blm10 is a monomeric structure with conserved C-terminal YYX motifs. The work done by Dange and colleagues revealed that Blm10's penultimate tyrosine is essential for core particle activation. This suggested that Blm10's YYX motif is functionally similar to the HbYX motif found in AAA-ATPases. Additionally, to support the notion that Blm10 is an activator, Blm10-20S proteasomes were shown to degrade peptides as well as an unstructured protein, tau-441 (Dange et al, 2011).

In addition to being an activator, Blm10 has been shown to be important in the late stages of core particle maturation. Like many chaperone proteins in yeast, the deletion of the *BLM10* gene does not have any obvious phenotypical defects in CP maturation (Marques et al, 2007). However, if the *BLM10* deletion is made in the presence of a mutant that disrupts the association of the 19S RP with 20S CP, defects in 20S CP assembly are observed (Marques et al, 2007). In addition, Blm10 has been associated with 15S intermediates (Li et al, 2007). This suggests that Blm10 has chaperone like activity during the assembly process.

1.7 Chaperone Proteins

Even though many details behind the structure and function of the 26S have been revealed, aspects behind the assembly of this structure remain unknown. Studies in yeast and mammalian cells have illustrated 20S assembly as a regulated process that involves at least six chaperone proteins in *Saccharomyces cerevisiae*: Ump1, potentially Blm10 (mentioned in the previous section), Pba1, Pba2, Pba3, and Pba4.

1.7.1 Ump1

Ump1 (ubiquitin-mediated proteolysis) protein was the first proteasome chaperone to be identified and characterized (Ramos et al, 1998). Ump1p was identified through a screen detecting mutants defective in degrading test substrates. The laboratory that discovered Ump1p demonstrated through pull-down experiments that Ump1p associates with 20S proteasomal precursors that contain β subunits with unprocessed N-terminal propeptides (Ramos et al, 1998). Later, others explicitly demonstrated that Ump1p is found on precursors containing a full α-ring with at least three β-subunits: β2, β3, and β4 (Li et al, 2007). Ump1p ensures that all of the β subunits are present before two half-proteasomes will dimerize. After dimerization, Ump1p becomes encapsulated in the central cavity and, as the β subunit propeptides are cleaved, Ump1p then becomes the first substrate to be degraded by the 20S proteasome (Ramos et al, 1998).

When *UMP1* is deleted there is an apparent defect in proteasome maturation. Not only are there fewer 20S and 26S proteasomes in *UMP1* deleted cells, but also there is an accumulation of proteasomal precursors. Oddly, these Ump1p lacking precursors had chymotrypsin-like activity. Normally this activity is seen in β5 only after the proteasome is fully assembled and the propeptides have been cleaved. The activity of β5 in proteasomeal precursors lacking Ump1p suggests that Ump1p may normally inhibit the autocatalytic activity of β5 (Ramos et al, 1998). More recently another group proposed that β5 propeptide helps drive the dimerization of two half-proteasomes while Ump1p acts as a checkpoint hindering this process until β7 is in place (Li et al, 2007).

1.7.2 Pba1-Pba2

Hirano et al, (2005) characterized PAC1 (Proteasome Associated Chaperone 1) in mammalian cells along with a second protein, PAC2. This group observed PAC1 and PAC2 as a complex that co-precipitated with tagged proteasome subunits. Additionally, through glycerol gradient centrifugation, this dimer was identified on early proteasomal precursors containing hUmp1 (human Ump1 protein) and in lighter fractions that lacked hUmp1 (Hirano et al, 2005). Immunoblots of the fractionated proteins suggested that PAC1 and PAC2 associate with α-rings and may promote α-ring assembly. Furthermore, immunoblot analysis of the lighter fractions suggested that PAC1 and PAC2 associate with the α5 and α7 subunits early in assembly (Hirano et al, 2005). Next, this group knocked down PAC1 and PAC2 in mammalian cells. The knockdown caused a shift of α

subunits from fractions corresponding to α-rings to fractions of much higher (i.e. nearly double) molecular mass. The authors reported that these higher molecular mass complexes were off-pathway intermediates, more specifically α-ring dimers (Hirano et al, 2005).

The gene encoding PAC2 was reported to have weak homology with *ADD66* (*YKL206C*) in yeast (Hirano et al, 2005). Add66 protein was characterized in yeast as having a role in ERAD (Endoplasmic Reticulum-associated degradation) (Scott et al, 2007). Comparing chymotrypsin like activity, *ADD66* mutants had reduced proteasome activity relative to wild-type cells. The mutant cells accumulated polyubiquitinated proteins and 20S CP intermediates (Scott et al, 2007). This group created a plasmid with *ADD66* C-terminally tagged to a *myc* epitope. When this plasmid was transformed into the mutant strain, polyubiquitinated proteins no longer accumulated. Lastly, this group suggested that the Add66p is degraded by the 26S proteasome (Scott et al, 2007). Scott and colleagues were the first to demonstrate Add66p as a protein that facilitates proteasome activity and assembly. The results from this study are interesting because this group C-terminally tagged Add66p and demonstrated that this tagged protein could relieve mutant phenotypes observed in *ADD66* mutants. It is now known that the C-terminus of the Add66 (now called Pba2) protein is important for 20S binding (see below) and the presence of a C-terminal epitope tag might interfere with this binding. Therefore, Add66p-*myc* may not fully behave like Add66p wild-type.

Similar to the mammalian orthologs, yeast proteasome chaperone proteins Pba1 and Pba2 have been characterized as a heterodimer that is found exclusively on proteasomal precursors (Li et al, 2007). Often times these precursors contain the Ump1 chaperone protein. Little is known about the specific function of the Pba1p-Pba2p. In order to assess the functional importance of a protein, deletions or mutations are often made. Interestingly, *pba1Δ, pba2Δ*, or *pba1Δpba2Δ* yeast strains appear to grow as well as wild-type cells (Li et al, 2007). However, if these deletions are combined with other mutations that affect proteasome function, such as an *RPN4* deletion, severe growth defects are observed. Rpn4p is a transcription factor that regulates proteasome expression levels (Xie & Varshavsky, 2001). Even though no growth defects are seen in *pba1Δ* and *pba2Δ* mutant strains, they do demonstrate a weak 20S assembly defect (Li et al, 2007). Li et al (2007) demonstrated that pba2Δ cells had reduced levels of propeptide processing.

Recently, archaeal orthologs of Pba1p and Pba2p were identified in the mesophilic methanogen *Methanococcus maripaludis,* PbaA and PbaB respectively (Kusmierczyk et al, 2011). As previously mentioned, archaeal α and β subunits will self assemble into 20S core particles when heterologously co-expressed in *E.coli* (which do not contain 20S proteasomes), therefore until this finding it was assumed that archaeal proteasome biogenesis did not require chaperone proteins. An *in vitro* study demonstrated that these chaperone proteins associate with proteasomal precursors in the same manner as their eukaryotic orthologs (Kusmierczyk et al, 2011).

Where Pba1p and Pba2p bind on the 20S CP is still up for debate. As previously mentioned, Hirano et al, (2005) suggested that the mammalian orthologs to these chaperone proteins associated with α5 and α7. However, a recent study by Park et al, (2011) suggested another set of α subunits. Park and colleagues set out to observe the interface between the 19S RP and the α-ring of the 20S CP. In this study mutations were made to the intersubunit pockets of the α-ring, so that the normal salt bridge formed between the Rpts of the 19S and the conserved lysine residue of the α subunits would be disrupted. When this group performed mass spectrophotometry on purified proteasome precursor complexes isolated from these lysine mutants, they revealed that the α5 mutant had significantly less Pba1p-Pba2p present, and α6 mutant had very little Pba2p present and no detectable Pba1p (Park et al, 2011). This result suggested that Pba1p and Pba2p may be interacting with α5 and α6.

1.7.3 Pba3-Pba4

The next proteasome assembly factor was identified in mammalian cells, PAC3. It was characterized through glycerol gradient centrifugation as being present in fractions lighter than those containing half-proteasomes (Hirano et al, 2006). Immunoprecipitation experiments strongly suggested that PAC3 is a component of α-rings, and *in vitro* binding assays suggested that it binds to one α subunit, α2, but it can bind to several of the β-subunits (strongly to β3 and β4 and weakly to β1 and β2) (Hirano et al, 2006). Furthermore, knockdown experiments suggested that PAC3 is involved in α-ring assembly (Hirano et al, 2006).

Shortly after the first characterization of PAC3, Le Tallec et al, (2007) published data characterizing four chaperone proteins in yeast, which they referred to as Poc1-4p. They characterized PAC1, PAC2, PAC3, and the uncharacterized PAC4 as being the mammalian homologs of the Poc1-4 proteins found in yeast (Le Tallec et al, 2007). Poc3p and Poc4p were shown to bind/interact with one another. When these proteins were individually expressed in *E.coli*, they were insoluble, however when co-expressed these proteins became soluble, strongly indicating an interaction between the two proteins. *E.coli* lysate co-expressing his-tagged Poc3p and Poc4p was run over a Ni-column and analyzed by gel filtration. A 40 kDa complex was observed, the Poc3p-Poc4p heterodimer (Le Tallec et al, 2007).

Shortly after the Poc3p and Poc4p heterodimer was identified, two groups independently identified this chaperone and published data on the functionality and localization of this heterodimer, which they called Pba3p-Pba4p and Dmp1p-Dmp2p, respectively (Kusmierczyk et al, 2008 and Yashiroda et al, 2008). It was shown that these proteins are responsible for ensuring that the α3 subunit is placed in-between α2 and α4. The deletion of *PBA3* and *PBA4* genes in yeast does not cause any growth defects at 30 °C, however they have mild temperature sensitivity as well as a hypersensitivity to canavanine. Like other Pba chaperone proteins previously mentioned, when the *pbα3Δpbα4Δ* strain was combined with another mutation, such as a point of function mutation in α5-*doα5,* the yeast had severe growth defects. Pull-

down assays suggest that the Pba3p-Pba4p complex associates with α5 and possibly α1 (Kusmierczyk et al, 2008).

Another group published data on the crystal structure of the Pba3p-Pba4p heterodimer (they referred to these proteins as Dmp1 and Dmp2) (Yaroshida et al, 2008). Even though this group stated that there was no sequence similarity between Dmp1p and Dmp2p to PAC3, they did mention that the structure was similar to PAC3. Yaroshida et al, (2008) demonstrated that Pba3p-Pba4p heterodimer could interact with α5 and α6. Additionally this group solved a co-crystal structure of Pba3p-Pba4p-α5 (Yashiroda et al, 2008). This structure explicitly demonstrated how this heterodimer interacts with specific non-conserved residues found only in the α5 subunit.

1.8 Unanswered Questions

Although many questions remain with respect to proteasome assembly and the role of 20S assembly factors, this thesis will focus specifically on the Pba1-Pba2 protein complex. Despite two different studies suggesting that Pba1p and Pba2p associate with specific α subunits, α5 and α7 (Hirano et al, 2005) and α5 and α6 (Park et al, 2011), no study to date has shown definitively where Pba1p and Pba2p bind on the 20S CP intermediates. Recently, a group revealed how Pba1p and Pba2p bind to the 20S CP. This group demonstrated that Pba1p and Pba2p contain functional C-terminal HbYX motifs. These HbYX motifs are essential for binding, contribute to assembly *in vivo*, and are partially redundant with one another (Kusmierczyk et al, 2011). Until this recent characterization of Pba1p and Pba2p, C-terminal HbYX motifs were thought to be an

exclusive feature of proteasomal activators, such as 19S, Blm10, and PAN. Since Pba1p and Pba2p contain HbYX motifs, they should bind to the same intersubunit pockets as activator HbYX motifs (Kusmierczyk et al, 2011).

Additionally, Kusmierczyk et al, (2011) characterized PbaA, an archaeal ortholog of Pba1p. PbaA was shown to bind to the same α-ring intersubunit pockets as proteasomal activators via its own C-terminal HbYX motif. This data all the more suggests that Pba1p and Pba2p will bind to the intersubunit pockets of the α-ring. I hypothesize that Pba1p and Pba2p each bind to specific α intersubunit pockets on 20S CP intermediates via C-terminal HbYX motifs. This work aims to physically demonstrate with which pockets Pba1p-Pba2p interacts.

CHAPTER 2. MATERIALS AND METHODS

2.1 Yeast Strains and Media

Yeast manipulations were carried out according to standard protocols (Guthrie, 1991). The strains used in this study are listed in Table 1. For plating and cultures yeast were grown in rich medium (YPD) or minimal medium (SD-Ura, SD-Trp, SD-Ura-Trp). For dilution series, cultures were grown overnight and diluted to an OD_{600} of 0.3. Six-fold dilutions were prepared in water and spotted onto selective media. Plates were incubated at 30 °C or 37 °C for three days.

The plasmids used in this study are listed in Table 2. The α subunit plasmids for *SCL1, PRE8, PRE9, PRE6, PRE5,* and *PRE10* genes (α1, 2, 3, 4, 6, and 7, respectively) were purchased from OpenBiosystems. The *PRE9* (α3) plasmid was received as a yeast stock, and it was extracted from yeast and transformed into Top10F' competent *E.coli* cells. The *PUP2* gene (α5) was cut from plasmid AKB35 with BsrGI and XbaI enzymes and pasted into similarly cut BG1805 vector. In α subunits 2-7 the conserved lysine residue (K66) was mutagenized to a cysteine by Quickchange mutagenesis (Stratagene). The α1 subunit has a tyrosine residue at the K66 position, and it was also mutagenized to a cysteine by Quickchange mutagenesis. Each of the plasmid-borne α subunits contains a C-terminal tandem affinity purification (TAP) tag, and the plasmids themselves contain a

URA3 gene, enabling selection on SD-Ura media. The X residue of Pba1p and Pba2p HbYX motifs were both mutagenized to cysteine residues. In brief, the C-terminal end of the wild-type *PBA1* plasmid (AKB495) was PCR amplified to mutagenize the I276 residue to a cysteine. The PCR fragment was ligated into plasmid AKB495 digested with XhoI and SacI, thereby replacing the wild-type C-terminus with a mutant fragment. To create the Pba2p HbYX mutant, Quickchange mutagenesis was performed. For this mutagenesis primers were designed with a point mutation to change the N267 residue on *PBA2* to a cysteine. The *PBA2* plasmid (AKB490) was used as template to create the HbYX mutant constructs containing a cysteine residue at the N267 position. DNA sequences were verified by DNA sequencing. Both *PBA1* and *PBA2* are expressed from their endogenous promoters. In addition, Pba1p is N-terminally tagged with the Flag epitope and Pba2p is N-terminally tagged with a hexahistidine (his) tag.

2.2 Galactose Inductions

Yeast cultures were grown in selective media overnight (SD-Ura-Trp). The OD_{600} was measured, and the appropriate amount of culture to make a 0.2 OD_{600} dilution in 50 ml was centrifuged in a 1.5 ml Eppendorf tube at 5,000 × *g* for 5 minutes. The cells were washed with 1 ml of ddH_2O and centrifuged again for one minute at 5,000 × *g*. The cells were then suspended in 1 ml of SDG-Ura-Trp, which is identical to SD-Ura-Trp except galactose rather than glucose is used as the carbon source. The suspension was then added to 49 ml of SDG-Ura-Trp in a 250 ml flask. The cultures were shaken at 30 °C for 18-24 hours before harvesting for disulfide crosslinking.

2.3 Disulfide Engineering of Pba1p and Pba2p to α Subunits

Crosslinking of Pba1p and Pba2p cysteine mutants to engineered cysteine residues at the base of α intersubunit pockets was carried out essentially as described (Velichutina et al, 2004), except that in some cases the cross-linking agent BMOE (Thermo Scientific) was used instead of $CuCl_2$ to generate crosslinks (Tian et al, 2011).

In brief, overnight yeast cultures expressing engineered cysteine residues were diluted to an OD_{600} of 0.3, and the cultures were incubated on a rolling drum at 30 °C until an OD_{600} of 0.8-1.2 was reached. The cultures were spun down in a falcon tube at 4800 × *g* for 5 minutes. The supernant was poured off, and the pellet was resuspended in 1 ml of ice cold water then transferred into a 1.5 ml Eppendorf tube. The suspension was centrifuged at 5,000× *g* for 1 minute. The supernant was removed then the pellet was resuspended in 100 µl of zymolyase buffer (1.2 M sorbitol, 50 mM Tris-HCl, pH 8.0, 0.5 mM $MgCl_2$) supplemented with 30 mM DTT. After incubating at room temperature for 15 minutes, the Eppendorf tubes were centrifuged. The supernant was removed and the pellet was resuspended in 100 µl of zymolyase buffer plus 4 µl of 15 mg/ml zymolyase. The reaction was incubated on a roller at 30 °C. After 30 minutes, the samples were centrifuged at 3500 rpm for 5 minutes at room temperature. Next, the supernant was removed and the cells were washed in 500 µl of zymolyase buffer. After another 5 minute centrifugation, the supernant was removed and 100 µl of lysis buffer (50 mM HEPES, pH 7.5, 1mM EDTA, 0.1% Trition-X100) supplemented with 1 µl of protease inhibitor cocktail (Thermo Scientific, Catalog# 87785) was added. Each

reaction was vortexed at top speed for 30 seconds and then placed on ice for 1 minute; this step was repeated 3 times. The Eppendorf tubes were then centrifuged at 15,000 rpm for 10 minutes at room temperature. The supernant was aspirated with a P200 Pipetteman and placed into a fresh Eppendorf tube.

Alternatively, yeast cell lysis was performed via bead beating. Briefly, the cells were harvested at an OD_{600} of approximately 1. The cells were pelleted by centrifuging at 5,000 × *g* or 5 minutes. The supernant was removed, and the cells were washed with 1 ml of ice-cold ddH_2O. The cells were pelleted again, and resuspended in 300 µl of chilled lysis buffer (50 mM Hepes, pH 7.5, 5 mM $MgCl_2$, 1 mM DTT). Approximately 100 µl of acid washed glass beads were added to the Eppendorf tube, and the tubes were vortexed on high for 3 × 3 min with three minute intervals on ice in-between each round of vortexing. The Eppenorf tubes were then centrifuged on high for ten minutes at room temperature. The supernant was removed and placed into a fresh Eppendorf tube for subsequent crosslinking.

Crosslinking was induced with 0.2 mM $CuCl_2$ at room temperature (Velichutina et al, 2004) or on ice with 0.1 mM BMOE purchased from Thermo Scientific (Tian et al, 2011). At 60 minutes 10 µl of Stop Solution (10 mM sodium iodoacetate and 50 mM N-ethyl maleimide) were added to the 100 µl lysate of $CuCl_2$ reaction and placed on ice. The BMOE reactions were quenched with 10 mM of DTT. Prior to adding BMOE to the control samples, 1 mM ATP and 5 mM $MgCl_2$ were added to the lysate and incubated at room temperature for 30 minutes.

2.4 Pull-down Assays

After crosslinking, some samples were subjected to immunoprecipitation with M2 Flag Resin (Sigma Aldrich) or applied to His SpinTrap Ni-NTA Columns (GE Healthcare).

Immunoprecipitations with M2 Flag resin were performed using 40 µl of gel suspension. The resin was first pelleted at 8,200 × *g* for 30 seconds, and the supernatant was removed. Before adding the lysate to the resin, the resin was washed twice with TBS. If the cells were lysed via spheroplast lysis method, then 80 µl of the 100 µl lysate was incubated with the resin for 2 hours to overnight at 4 °C while rotating gently. Or if the bead beading lysis method was performed, then 280 µl of the 300 µl lysate was added to the resin for 2 hours to overnight at 4 °C. After incubating the lysate with the resin, the Flag-tagged protein was recovered by first pelleting the resin and removing the supernatant, then washing the resin three times with 600 µl of TBS. The Flag-tagged proteins were recovered by boiling the resin in 20 µl of 2x sample buffer or eluting in 100 µl of flag peptide (450 ng/µl) for 2 to 4 hours at 4 °C while rotating gently.

Sample application to 100 µl Ni-NTA columns was carried out as follows. First, the columns were cleared of storage solution by centrifuging the column at 100 × *g* for 30 seconds. Next, the column was washed twice with 600 µl binding buffer (50 mM Hepes-NaOH; pH 7.5, 150 mM NaCl, 5 mM $MgCl_2$, 40 mM imidazole). After washing the resin, the lysate was added to the beads, and centrifuged again. The flow through was discarded, and the column was washed three times with 600 µl of binding buffer.

Finally, the sample was eluted in 400 µl of elution buffer (50 mM Hepes-NaOH; pH 7.5, 500 mM NaCl, 5 mM $MgCl_2$, 500 mM imidazole).

2.5 TCA (Trichloroacetic Acid) Precipitation

Eluted samples were concentrated by TCA precipitation. For each eluted sample, trichloroacetic acid was added to a final concentration of 10%, and the sample was incubated at 4 °C for 15 minutes. Samples were centrifuged at 23,000 rpm for 10 minutes to pellet the protein. The supernant was removed, and the pellet was washed 3 times with ice-cold acetone. After the last wash, the supernant was removed, and the pellet was further dried at 100 °C for 10 minutes.

2.6 SDS-PAGE and Western Blot Analysis

For the analysis of the disulfide crosslinked Pba1p to α6 and Pba2p to α7, SDS-PAGE and Western blot analysis was carried out as described (Chen and Hochstrasser, 1995). Laemmli (2x) sample buffer supplemented with 0.02 % sodium iodoacetate, 0.3 % SDS, 4 % glycerol, 3.2 mM Tris-HCl, pH 6.8, and a trace of Bromophenol Blue powder was added to each sample. Samples were applied to 8 or 12 % SDS-PAGE gels and electrophoresed at 80 V until the dye front ran off the bottom of the gel. The proteins on the gels were transferred to Immobilon membrane (Millipore) by semi-dry or wet-transfer methods. The semi-dry transfer was carried out on a Bio-Rad Trans-Blot. For the semi-dry method a tris-gylcine transfer buffer (25 mM tris, 192 mM glycine, and 20% methanol) was used. The trans-blot was run at 15 V for 26 minutes. For wet transfers the Bio-Rad Mini Trans-Blot Electrophoretic Transfer Cell was used. Wet transfers were

performed in essentially the same transfer buffer as previously described except without methanol. The transfer was run 130 minutes at 25 V. Immediately after transfer, the membrane was blocked in a 5 % non-fat milk-TBS solution overnight at 4 °C. For western blot analysis, the following primary antibodies were used: anti-hemagglutinin (MP Biomedical, Catalog# 632191), peroxidase anti-peroxidase complex, or PAP, (Sigma, Catalog# P1291), anti-tetra-his (Qiagen, Catalog# 34670), and an anti-Flag (Sigma, Catalog# F1804). Proteins with hemagglutinin (HA) and Flag were visualized with horseradish peroxidase-coupled secondary antibody, Goat Anti-Mouse (SouthernBiotech, Catalog# 1070-05). The dilutions used for each antibody are listed on Table 3. The membrane was exposed to CL-X Posure Film (Thermo Scientific, Catalog# 34091) from 10 seconds to 15 minutes, then immediately developed.

CHAPTER 3. RESULTS

3.1 Rationale

The proposed work aims to determine which α intersubunit pockets the Pba1p-Pba2p complex interacts with on the 20S CP. As mentioned earlier, HbYX motifs of 20S activators insert into α intersubunit pockets resulting in the formation of a salt-bridge between the C-terminal carboxylate of the HbYX motif and a conserved lysine (K66 in *T. acidophilum*) at the base of this pocket (Figure 3). Given that Pba1p-Pba2p both contain functional HbYX motifs (Kusmeirczyk et al, 2011) and that these motifs have been shown to be necessary for binding to 20S (Kusmeirczyk et al, 2011), I reasoned that a crosslinking approach might be a reasonable means of detecting Pba1p-Pba2p-20S interaction. In this approach (Figure 4), the C-terminal residue of the HbYX motif in either Pba1p or Pba2p is mutated to a cysteine, as is the pocket lysine. When the two complexes interact in the presence of mild oxidizing conditions, a crosslink (disulfide bond) should be formed between the engineered cysteine residues.

3.2 Mutagenesis

In order to conduct the crosslinking assay, QuickChange Mutagenesis was performed to mutate the conserved α subunit pocket lysine residue (Figure 5) to a cysteine. The α1 subunit is the only α subunit that lacks the conserved lysine residue.

Instead of a lysine at the conserved position (K66 in *T. acidophilum*), it contains a tyrosine residue. For completeness, this tyrosine was mutagenized to cysteine. All 14 α subunit plasmids (seven wild-type and seven lysine mutants), are controlled by a galactose-inducible promoter and contain a C-terminal Tandem Affinity Purification (TAP) tag.

In addition to the α subunit mutations, *PBA1* and *PBA2* HbYX motifs were mutagenized. The wild-type *PBA1* plasmid used was previously constructed with an N-terminally Flag-tagged Pba1p expressed from its endogenous promoter. Primers were designed to mutate the HbYX motif, X residue (I276) on Pba1p to a cysteine. Using the wild-type plasmid as template, a C-terminal fragment of *PBA1* was amplified containing this mutation. This C-terminal fragment was cut and ligated into a similarly digested wild-type plasmid, creating the HbXY mutant plasmid, *pba1-C*. The wild-type *PBA2* plasmid contained an N-terminally his-tagged Pba2p expressed from its endogenous promoter. The HbYX motif, X residue (N267), on *PBA2* was mutagenized to a cysteine via QuickChange Mutagenesis creating *pba2-C* plasmid.

Once the *pba1* and *pba2* HbYX mutant plasmids were generated, I wished to demonstrate that the mutations would not affect Pba1p-Pba2p function. The usual means to do this would be to demonstrate that the mutants are capable of fully complementing *pba1Δ* and *pba2Δ* yeast strains. However, as previously mentioned, *pba1Δ, pba2Δ*, or *pba1Δpba2Δ* do not have any obvious growth defects (Li et al, 2008). Therefore, in order to test if the *pba1-C* or *pba2-C* mutants affected the growth of yeast,

these mutants were transformed into *pba1Δ* or *pba2Δ* strains that also contained a deletion of the *RPN4* gene. Rpn4p is a transcription factor that regulates proteasome expression levels (Xie et al, 2001). As seen in Figure 6, the *rpn4Δ* deleted yeast cells themselves have a very mild growth defect at 37 °C. However, when the *rpn4Δ* was combined with the *pba1Δ* or the *pba2Δ* the yeast cells were no longer viable at 37 °C. When wild-type *PBA1* and *PBA2* were transformed into their respective double mutants, growth of the double mutants at 37 °C was restored. When the *pba1-C* and *pba2-C* mutants were transformed into their respective double mutants, each HbYX mutant was also able to restore the growth to the same extent as the wild-type proteins (Figure 6). This suggested that mutation of the X residue on the HbYX motifs of Pba1p or Pba2p did not affect Pba1p-Pba2p function.

3.3 Detecting Crosslinks with HbYX mutants

Eukaryotic proteasomes contain seven unique α subunits; therefore, there are seven possible pockets to which Pba1p and Pba2p can bind. I relied on previously published data to initially focus my search on likely interacting partners. Specifically, Hirano et al. (2005) had shown that the mammalian orthologs of Pba1p-Pba2p, PAC1-PAC2, interacted with α5 and α7. More recently, Park et al, (2011) suggested that Pba1p-Pba2p might be interacting with the lysines on α5 and α6. Therefore, the first series of experiments were performed using crosslinkable Pba1p and α6. Unless noted otherwise the following experiments were performed in at least triplicate and the data shown are representative blots.

3.4 Pba1p-α6 crosslinking

To detect interaction between Pba1p and α6, specifically the α5-α6 intersubunit pocket, I transformed *pba1Δ* yeast with plasmids encoding *pba1-C* and α6-TAP and generated whole cell lysates from 5 ml cultures. Crosslinking was initiated by the addition of $CuCl_2$ and after 60 minutes, aliquots were withdrawn and analyzed by immunoblot with anti-PAP. Immunoblot analysis detected the predicted α6 TAP-tagged species at approximately 44 kDa (Figure 7A, lanes 1-4, 9). However, incubation of whole cell lysates in $CuCl_2$ did not stimulate a detectable disulfide formation between Pba1p and α6 (Figure 7A, lanes 1-4)

Even though no crosslinking was observed in the lane with crosslinkable Pba1p and crosslinkable α6, this was not due to the failure of the crosslinking method itself because crosslinking was observed in the relevant control samples (Figure 7B). The control strains for this experiment were obtained from another study that identified α4 as the α subunit that replaces α3 when α3 (the only non-essential 20S proteasome subunit in yeast) is deleted (Velichutina et al, 2004). In that study, a hexa-histidine tagged (his-tagged) α4 subunit was engineered with two cysteine residues that would be in close proximity to one another if and only if two α4 subunits were positioned next to each other in the same α ring. Under mild oxidizing conditions, the α4-α4 crosslinked species is easily detected in *α3Δ* yeast, and this interaction was shown to be sensitive to reducing agents. By contrast, wild-type yeast (i.e. α3, not *α3Δ*) with crosslinkable α4 treated under the same mild oxidizing conditions do not yield the α4-α4 crosslinked

species because in these yeast the α3 subunit assumes its normal place within the α-ring (Veluchitina et al, 2004). As predicted, I observed that $CuCl_2$ incubation of whole cell lysates stimulated disulfide bond formation between crosslinkable α4 subunits in *α3Δ* yeast (Figure 7B, + lane), and this α4-α4 crosslinked species was reduced in the presence of DTT (Figure 7B, + DTT lane). As expected, the crosslinkable α4 subunits did not crosslink in wild-type yeast cells (Figure 7B, - lane). Thus I conclude that the failure to detect Pba1p-α6 crosslinks was not due to the failure of the assay per se. Instead, the failure was likely due to suboptimal conditions for this particular protein pair, and I decided to modify my protocol in a number of ways in an attempt to optimize the assay conditions.

3.4.1 Increasing Culture Size

One possibility for the failure to observe Pba1p-α6 crosslinks is that the crosslinked species is of low abundance. I decided to repeat the analysis using increased culture volumes. Anti-PAP immunoblot analysis was performed on $CuCl_2$ treated whole cell lysates from 10 ml yeast cultures (2-fold increase from the previous experiment) prepared in the same manner as before. Incubation of cell extracts in $CuCl_2$ did not stimulate a detectable disulfide formation between Pba1p and α6 (Figure 8A, lanes 1-4). Anti-PAP immunoblot analysis detected the predicted α6 TAP-tagged species at approximately 44 kDa (Figure 8A, lanes 1-4, 9), but did not detect any bands at the predicted crosslinked species size, 75 kDa.

Even though no crosslinking was observed in the anti-PAP immunoblot analysis, the assay again was performed correctly as demonstrated by the positive and negative crosslinking controls. $CuCl_2$ incubation of whole cell lysates stimulated disulfide bonds between crosslinkable α4 subunits in $\alpha 3\Delta$ yeast (Figure 8B, + lane), and this α4-α4 crosslinked species was reduced in the presence of DTT (Figure 8B, + DTT lane). The crosslinkable α4 subunits did not crosslink in wild-type yeast cells (Figure 8B, - lane).

The above analysis was repeated with whole cell lysates obtained from 50 ml cultures. Incubation of cell lysates in $CuCl_2$ did not stimulate a detectable disulfide formation between Pba1p and α6 (Figure 9A, lanes 1-4). Anti-PAP immunoblot analysis detected the predicted α6 TAP-tagged species at approximately 44 kDa (Figure 9A, lanes 1-4, 9), but did not detect any bands at the predicted crosslinked species size, 75 kDa.

Although the Pba1p-α6 crosslinked species was not observed in the anti-PAP immunoblot analysis, the assay was performed correctly as demonstrated by the positive and negative crosslinking controls as described above (Figure 9B).

3.4.2 Larger Cultures and MG132

After not observing a crosslink in the lysate from 50 ml cultures, the next set of experiments focused on increasing the binding affinity of Pba1p to the 20S core particle intermediates. Prior to crosslinking, the lysate was incubated in proteasome inhibitor MG132. Proteasome inhibitor MG132 is a reversible inhibitor that blocks the chymotrypsin like activity of the proteasome. Other groups have demonstrated that proteasome inhibitors increase the binding affinity of Pba1p and Pba2p to the 20S

proteasome (Hirano et al, 2005 and Kusmierczyk et al, 2011). I reasoned that it might be possible to increase crosslinking efficiency by boosting the affinity of 20S for Pba1p by using MG132.

Prior to incubating the lysate in $CuCl_2$, the lysates were incubated in 20 µM MG132. Anti-PAP immunoblot analysis was carried out on the MG132 treated crosslinked lysate as described above. Although no clear bands were observed that would suggest the formation of a Pba1p-α6 crosslink, the $CuCl_2$ may have stimulated the formation of disulfide-linked species because several faint (non-specific) bands are seen between the 50 kDa and the 75 kDa markers (Figure 10A, lanes 1-4). Interestingly, these bands are present in all of the lanes, including those with wild-type Pba1p and α6. These bands disappeared in the presence of DTT (Figure 10A, lane 9) consistent with them being the result of some kind of disulfide-linked species.

The crosslinkable α4 control samples indicated that the crosslinking assay was performed accurately. $CuCl_2$ incubation of whole cell lysates stimulated disulfide bonds between crosslinkable α4 subunits in *α3Δ* yeast (Figure 10B, + lane), and this α4-α4 crosslinked species was reduced in the presence of DTT (Figure 10B, + DTT lane). The crosslinkable α4 subunits did not crosslink in wild-type yeast cells (Figure 10B, - lane).

3.4.3 50 ml Cultures, MG132, and Flag Pull-Down

The next set of crosslinking experiments used lysate obtained from 50 ml cultures and, similar to Figure 10A, these samples were incubated with proteasome inhibitor MG132. However, I decided to combine this experimental set up with a Flag

pull-down. In previous experiments, only 20 µl of the 100 µl of whole cell lysate used in the crosslinking experiment could be loaded onto the gel at any one time due to volume constraints of the well. By carrying out an immunoprecipitation first, I should be able to isolate all of the Pba1p protein in those 100 µl of lysate and load all of it onto the gel. This should further increase the odds of detecting a crosslinked species.

Anti-flag immunoprecipiations were performed on inhibitor treated crosslinked lysates prepared as before (Figure 10A). The elutions were carried out using flag peptide. Additionally, the resin containing both crosslinkable Pba1p and α6 was boiled in sample buffer after the peptide elution. This was done to recover protein that may not have eluted off the beads as we routinely observe significant amounts of protein still attached to the resin even after eluting in peptide (not shown). Unfortunately, the elutions of the crosslinked lysate did not yield the expected flag-tagged Pba1p (Figure 11 and see discussion 4.1).

3.5 Pba2p-α7 Crosslinking

In parallel with the Pba1p-α6 crosslinking experiments, I attempted to visualize crosslinking between Pba2p and α7, more specifically the α6-α7 intersubunit pocket. These experiments were performed in duplicate and representative blots are shown.

Similar to the Pba1p and α6 assays, we transformed *pba2Δ* yeast with plasmids encoding *pba2-C* and α7-TAP and generated whole cell lysates from 5 ml cultures. Incubation of whole cell lysates in $CuCl_2$ did not stimulate a detectable disulfide

formation between Pba2p and α7 (Figure 12A, lanes 1-4). Anti-PAP immunoblot analysis detected the predicted α7 TAP-tagged species at approximately 50 kDa (Figure 12A, lanes 1-4, 9), but did not detect any bands near the predicted crosslinked species size, 80 kDa.

Although no crosslinking was detected via anti-PAP immunoblot analysis, the crosslinkable α4 control samples indicate the assay was performed correctly. $CuCl_2$ incubation of whole cell lysates stimulated disulfide bonds between crosslinkable α4 subunits in *α3Δ* yeast (Figure 12B, + lane), and this α4-α4 crosslinked species was reduced in the presence of DTT (Figure 12B, + DTT lane). As demonstrated in other studies (Velichutina et al, 2004), the crosslinkable α4 subunits did not crosslink in wild-type yeast cells (Figure 12B, - lane).

3.5.1 Attempts to Increase Crosslinking Efficiency and Detection

As with the Pba1p-α6 experiments described above, I next performed anti-PAP immunoblot analysis on whole cell lysates from 50 ml cultures. Visualizing the crosslinked lysate, the expected 50 kDa α7 TAP-tagged species was observed (Figure 13A, lanes 1-4). Interestingly, the sample containing crosslinkable α7 and wild-type Pba2p had several unidentified bands (Figure 13A, lane 2). Additionally the sample containing crosslinkable Pba2p and crosslinkable α7, also had several unidentified bands present (lane 4), albeit not to the same extent as lane 2 (Figure 13A). The high molecular weight bands present in lane 4 appear to be sensitive to reducing agent DTT

(Figure 13A, lane 7) suggesting that they are the result of a disulfide linked species. Unfortunately there was some difficulty processing the associated control samples. Namely, the crosslinked α4-α4 was visualized, arguing that the crosslinking assay was working, but the uncrosslinked α4 was not detected, perhaps suggestive of a blotting problem in this instance (Figure 13B).

The next series of immunoblot experiments were performed using lysate extracted from 50 ml cultures and incubated with proteasome inhibitor MG132 prior to crosslinking. Moreover, the lysate was applied to a Ni-NTA column in order to increase recovery of Pba2p, based on the same reasoning for carrying out the anti-Flag pull downs of Pba1p. Anti-PAP immunoblot analysis of the total fractions indicated that the samples were loaded in similar amounts (Figure 14A). Although I did not observe the expected crosslinked species in the elute fractions from the Ni-NTA column, anti-PAP immunoblot analysis revealed that mutant α7 was pulled down by both the wild-type and crosslinkable his-tagged Pba2p (Figure 14B). The α7-TAP species should not bind the resin owing to the fact that it does not have any intrinsic affinity for this resin. Both wild-type Pba2p and the mutant Pba2p (N267C) pulled down the α7 mutant more efficiently than the wild-type α7 (Figure 14B). Even though a crosslinked species was not detected, the his-tagged α4 crosslinking controls demonstrated that the assay was performed correctly, as described in previous sections (Figure 14C).

3.6 Alternative Crosslinking Approach

The experiments mentioned above failed to detect the Pba1p-α6 and the Pba2p-α7 crosslinks. This may be a consequence of mutating the conserved lysine residue within the α intersubunit pocket. Mutating this residue to a cysteine may have decreased the affinity of Pba1p-Pba2p to the 20S CP. In addition to possibly decreasing the affinity, my initial approach neglected the endogenous cysteine residues on neighboring subunits. There is a cysteine residue on α5, which is within close proximity to the α5-α6 pocket, and there is another cysteine on α6, which is near the α6-α7 pocket. These endogenous cysteines may have interfered with Pba1p-α6 and Pba2p-α7 crosslinking.

To address these issues, a complementary crosslinking approach was undertaken based on yeast strains developed in the Finley laboratory. This laboratory developed an assay to determine which α intersubunit pockets were engaged by which HbYX motifs in Rpt subunits of the 19S. Their assay aimed to crosslink the 19S Rpt C-terminal tails to the α intersubunit pockets of the 20S CP. These strains, similar to the ones I developed, were engineered with crosslinkable α subunits; however, unlike my approach, the crosslinkable cysteine was placed on the side of the α intersubunit pocket (Figure 15), not at the base (Tian et al, 2011). By using the side of the pocket to crosslink, the conserved lysine residue at the base of the pocket remains intact. Additionally, this group mutated the endogenous cysteine residues on α5 and α6 to alanine residues in order to prevent any non-specific intra-subunit crosslinking. Moreover, this study used

crosslinker BMOE. BMOE, bis(maleimido)ethane, is a non-reversible crosslinker. This crosslinker has an advantage over $CuCl_2$. The BMOE molecule is structured so that it may crosslink cysteines that are too far apart to crosslink based on the direct formation of cys-cys disulfides under mild oxidizing conditions. BMOE contains two maleimide groups, one on each end of a spacer arm. The maleimide groups form stable thioether linkages to sufylhydryl groups.

Since the Finley lab demonstrated that 19S Rpt tails, especially those containing C-terminal HbYX motifs with engineered cyteines in the X position, could crosslink to these mutated pockets, I hypothesized that my engineered *pba1-C* and *pba2-C* will also be able to crosslink into these pockets. Therefore, the Finley yeast strains were transformed with either an empty vector or vectors containing wild-type *PBA1* or *pba1-C*. Additionally, these crosslinking assays were performed with crosslinker used in the Rpt crosslinking assay, BMOE.

3.6.1 Pba1p-α6 Crosslinking

Initially I attempted to observe crosslinks between Pba1p and α6. As before, whole cell lysates were extracted from 50 ml cultures and incubated with proteasome inhibitor MG132 prior to crosslinking. Crosslinking was induced with 10 μM BMOE. The crosslinked lysates were immunoprecipitated with M2 anti-Flag resin to isolate Pba1p, and the immunoprecipitates were analyzed by immunoblotting with anti-HA antibody (Figure 16). There appears to be a specific band just above the 25 kDa marker in the

pulldown lane with crosslinkable Pba1p (Figure 16, lane 6). Immunoblot analysis also detected a faint band at approximately 60 kDa in the *pba1-C* pull down lane, consistent with the position of a crosslinked species (Figure 16, lane 6). This band was not detected in the *PBA1* (WT) or empty vector pull down lanes. Unexpectedly, none of the relevant proteins within the total lanes (1, 3, and 5) were detected with antibody, even though protein is clearly present in the pull down lanes. This anomaly may be attributed to inefficient lysis of the yeast cells. If only a small fraction of the cells are being lysed, then the total fractions of the lysate may not contain enough protein for immunoblot detection. However, the pull down lanes contain concentrated amounts of flag-tagged eluted protein; therefore, proteins were detectable via immunoblotting.

To overcome possible lysis inefficiency, I decided to modify the analysis and switch the lysis method from spheroplasting to bead beating. Otherwise, the experiment was carried out as above. Western blot analysis of these immunoprecipitates did yield protein in the total lanes (Figure 17, lanes 1, 3, and 5) consistent with lysis being much more efficient. Moreover, specific bands were present in the wild-type Pba1p pull down lane (4) and the crosslinkable Pba1p pull down lane (6). Both of these lanes contain bands at approximately 30 kDa, which corresponds to the approximate size of 6×HA-tagged α6 protein. This suggests that Pba1p was able to pull down an α6-containing species in these samples. Unfortunately, the lane containing the crosslinkable Pba1p did not yield a band at the expected crosslinked size, 60 kDa (Figure

17, lane 6). Experiments to optimize the conditions using the Finley strains are continuing.

CHAPTER 4. DISCUSSION

The proteasome ubiquitin pathway has been shown to play an essential role in many highly regulated cellular processes, such as the cell cycle (reviewed by Hochstrasser, 1996). The function of the proteasome has been well characterized; however, much less is understood about the assembly of this structure. Studies over the past two decades have indicated that proteasome assembly is a highly regulated process. Within eukaryotes at least six assembly chaperone proteins have been identified: Ump1p, Pba1p, Pba2p, Pba3p, Pba4p, and potentially Blm10 (reviewed by Kusmierczyk & Hochstrasser, 2008).

My work focused on chaperone proteins Pba1p and Pba2p. These proteins were first characterized in a mammalian cell line (Hirano et al, 2005) and later in yeast (Li et al, 2007). These proteins were shown to have important roles in the early events of assembly (Le Tallec et al, 2007 and Li et al, 2007). Two different groups suggested which 20S subunits Pba1p and Pba2p could bind to; however, neither group explicitly demonstrated how this interaction was mediated (Hirano et al, 2005 and Park et al, 2011). Recently, Pba1p and Pba2p were shown to bind to proteasomal intermediates via their C-terminal HbYX motifs (Kusmierczyk et al, 2011). The mechanism by which HbYX motifs bind to proteasomes has been characterized in activators such as PAN

(Smith et al, 2007) and the 19S RP (Rabl et al, 2008). This C-terminal HbYX motif has been shown to insert itself within α intersubunit pockets. The carboxylate group of the X residue within the motif forms a salt-bridge with a conserved lysine residue within the base of the α intersubunit pocket (Smith et al, 2007). To identify precisely which α intersubunit pockets Pba1p and Pba2p bind, I attempted to trap this interaction using a crosslinking strategy. The X residues in the HbYX motifs of Pba1p and Pba2p were mutated to cysteines, which itself had no effect on the function of these two proteins (Figure 6). Similarly, each of the conserved lysine residues were also mutated to cysteines, and I attempted to induce cys-cys crosslinks by exposing the mutated proteins to mild oxidizing conditions.

Other studies have suggested that Pba1p-Pba2p may bind to α5, α6, or α7 (Hirano et al, 2005 and Park et al, 2011). Therefore, my experiments focused on identifying a crosslink between Pba1p-Pba2p and these α subunits.

4.1 Pba1p Crosslinking

Specifically, my initial experiments focused on detecting a crosslink between Pba1p and α6. Even though several attempts were made to optimize the crosslinking conditions between the two proteins, I was unable to detect the Pba1p-α6 crosslink. Initially, I looked at ways to increase the likelihood of detection. This was accomplished by supplementing the amount of Pba1p present in the assay. The number of Pba1p proteins present in the cell is approximately 1/10 of the α subunits (Ghaemmaghami et al, 2003). Since Pba1p is in such low abundance within the cell, the intensity of the

crosslinked signal will be weak. Therefore, if all of the Pba1p within the cell crosslinked to α6, the crosslinked signal detected via anti-PAP immunoblotting will only be 1/10 the intensity of the α6 signal. To increase the signal of the crosslink, I increased the protein concentration of the lysate 2-fold and then 10-fold. Unfortunately, the above conditions failed to detect the Pba1p-α6 crosslink, whereas the assay controls consistently produced a crosslink (Figures 9B and 10B).

The next approach taken to visualize the crosslink involved increasing the binding affinity of Pba1p to the 20S CP intermediates. Work done in yeast explicitly demonstrated that exposing lysate to proteasome inhibitor increased the binding affinity of chaperone proteins to the 20S CP (Kusmierczyk et al, 2011). The next series of experiments incubated the 10-fold concentrated lysate in proteasome inhibitor MG132, prior to crosslinking. Again, this approach failed to detect a clear crosslinked species; however, several faint bands were present in the lanes 1-4 (Figure 10A). When the crosslinked sample was exposed to DTT, the faint bands disappeared (lane 9), which strongly suggested that the faint bands seen in lanes 1-4 were induced by $CuCl_2$ crosslinking (Figure 10A). To determine if any of the faint bands observed were in fact the Pba1p-α6 crosslink, the next method used the proteasome inhibitor treated 10-fold larger lysate in combination with a Flag pull down. Unfortunately, elutions of this crosslinked lysate did not produce the crosslink or the expected flag-tagged Pba1p (Figure 11).

Despite attempts to optimize the crosslinking efficiency and detection, a clear crosslink was never observed. There are at least three possible explanations for why I was unable to detect the Pba1p-α6 crosslink. First, it is possible that the cysteines on the crosslinkable Pba1p and α6 were never close enough to crosslink with $CuCl_2$. Under normal conditions, the lysine at the base of the pocket forms a salt-bridge with the incoming C-terminal HbYX motif carboxylate. The lysine side chain has four methylene groups that allow the ε amino group to sit relatively high within the pocket. In contrast, when this lysine was mutated to a cysteine, the length of the side chain was reduced by three methylene groups; therefore, the corresponding sulfhydryl sits lower within the α intersubunit pocket. Perhaps this extra distance was far enough to prevent crosslinking between the engineered cysteine residues. Second, mutating the conserved pocket lysine residue to a cysteine may have decreased the binding affinity of Pba1p to the 20S CP. Therefore, if Pba1p is no longer interacting with α6, then the Pba1p-α6 crosslink will never be detected. Indeed, recent experiments by Park et al, (2011) show markedly decreased recovery of Pba1p on proteasome assembly intermediates containing a lysine-to-alanine mutation of the α6 pocket lysine, and my project was initiated prior to the publication of this study. Third, there is an endogenous cysteine residue on α5 that is within close proximity to the α5-α6 pocket. This endogenous cysteine may have formed an intra-molecular disulfide bond with the cysteine engineered in the base of the pocket. This would reduce the number of crosslinkable pockets available for Pba1p crosslinking.

4.2 Pba2p Crosslinking

In parallel to the Pba1p crosslinking, my work focused on identifying the α5, α6, and α7 intersubunit pockets as potential binding sites for Pba2p. Specifically, I focused on visualizing the Pba2p-α7 interaction.

Although several attempts were made to optimize crosslinking efficiency and detection, I failed to detect a Pba2p-α7 crosslink. Similar to Pba1p, there is a low abundance of Pba2p within the cell (Ghaemmaghami et al, 2003). Therefore, the crosslinked Pba2p-α7 band will not be easily detected. In order to increase the likelihood of detecting the Pba2p-α7 species, I extracted lysate from larger cultures to increase the amount of Pba2p within the lysate. When the lysate was concentrated 10-fold, several unexpected bands were detected via anti-PAP immunoblot analysis. The samples containing crosslinkable α7 had heavy banding patterns throughout the lanes. Even more surprisingly, the sample containing wild-type Pba2p and crosslinkable α7 had more high molecular weight bands present than the sample containing both crosslinkable species (Figure 12A). In short, the reason for this phenomenon is not clear, but these bands only occurred in the presence of a crosslinkable α7 subunit.

Since none of the high molecular weight bands observed in Figure 12A contained a clear Pba2p-α7 crosslink, the next approach, similar to attempts made in the Pba1p assays, focused on increasing efficiency of both crosslinking and detection. To increase the chances of crosslinking, the lysate was incubated in proteasome inhibitor MG132. As previously mentioned, proteasome inhibitors have been shown to increase the

binding affinity of chaperone proteins to the 20S CP (Kusmierczyk et al, 2011). Increasing the affinity of Pba2p to the 20S CP should increase the likelihood of trapping the Pba2p-α7 interaction via crosslinking. In order to more easily detect the Pba2p-α7 crosslink, the inhibitor treated crosslinked lysate was run over a Ni-NTA column, since Pba2p is N-terminally his-tagged. The total fractions of this crosslinking experiment (Figure 13A) yielded similar banding patterns observed in Figure 12A. When the elute fractions were analyzed by anti-PAP immunoblot, no crosslink was detected; however, α7 was present in the elute fractions (Figure 13B), and it appeared that his-tagged Pba2p, wild-type and crosslinkable, pulled down more crosslinkable α7 than wild-type α7. This suggests that Pba2p, both wild-type and crosslinkable, bound more tightly to the mutated α7 than wild-type α7.

Even though some of the Pba2p-α7 crosslinking assays had interesting results, the Pba2p-α7 crosslink was never detected. Similar to the Pba1p-α6 assays (mentioned above), there are at least three possible explanations for why I was unable to detect the Pba2p-α7 crosslink. First, it is possible that the engineered cysteines on Pba2p and α7 were never close enough to crosslink. Second, mutating this conserved lysine residue to a cysteine may have decreased the binding affinity of Pba2p to the 20S CP. As a result, if Pba2p is no longer interacting with α7, then the Pba2p and α7 will never crosslink. Third, there is an endogenous cysteine residue located on α6 that is within close proximity to the α6-α7 pocket (the Pba2p binding site) that could result in competing crosslinks.

4.3 A New Approach

While this project was in progress, another group published crosslinking data involving the interaction of the 19S Rpt C-terminal tails with the α intersubunit pockets of the 20S CP (Tian et al, 2011). As in my approach, this group took advantage of the known HbYX interaction. In this study the last residue of the C-terminal tails of the Rpt subunits were mutated to cysteines. In contrast to my approach, which mutated the conserved lysine residue at the base of the pocket to a cysteine, this group mutated a non-conserved residue on the side of the pocket, keeping the conserved lysine residue intact. Additionally, this group used crosslinker BMOE to induce the formation of a crosslink between the engineered cysteine residues.

By using these yeast strains to crosslink Pba1p and Pba2p to the 20S CP intermediates, the potential issues in the previous approach should be alleviated. In brief, these strains eliminated the issue of decreased binding affinity because the pocket lysine remains intact, and the issue of cysteine residue proximity was resolved by using a crosslinking agent with a long spacer arm. Additionally, the endogenous cysteines located near the potential Pba1p and Pba2p binding pockets were mutated to alanines. Considering these improvements, these strains are likely to crosslink with my engineered Pba1p and Pba2p proteins.

4.4 Detection Issues

Before discussing the results of the crosslinking conducted with the new strains of yeast, the detection issues that arose during the course of this project should be

noted. In the beginning of this project, there were no issues with detecting proteins via immunoblot analysis. However, detection issues arose when I ran out of the secondary antibody, HRP-conjugated Goat Anti-Mouse (IgGγ_1) and replaced it with a new aliquot from the same company. At that time, I suddenly had difficulty detecting flag-tagged proteins (Figure 11), and I was no longer able to clearly detect his-tagged proteins either (Figures 13B). This detection issue became even more apparent when immunoblot analysis of the crosslinked Finley strains began. These new strains relied on a secondary HRP-conjugated antibody to visualize the HA-tagged α subunits. After several weeks of troubleshooting, it was finally discovered that the newly purchased secondary was from a different production lot than the original batch, and this lot turned out to be not functional. New secondary antibodies have since resolved the detection issue; however, it took over a month to resolve, which negatively impacted progress of this project.

4.5 Pba1p-α6 Crosslinking (Finley Strains)

Crosslinking with the Finley strains was performed using concentrated lysate incubated in proteasome inhibitor MG132. Crosslinking was induced with BMOE, and after crosslinking total fractions were collected, and the remaining lysate was immunoprecpitated with M2 Flag resin. Oddly, no protein was detected in the total fractions; however, proteins were detected in the pull down lanes. Specifically, the pull down lane containing crosslinkable Pba1p had a band at approximately 60 kDa, which corresponds to the expected size of a Pba1p-α6 crosslinked species. This band was not present in the wild-type or empty vector pull down lanes. This furthermore suggests

that this band may in fact be the crosslinked Pba1p-α6. In addition to the 60 kDa band, a band at approximately 30 kDa was observed in the pull down lane with crosslinkable Pba1p. This may be the α6-HA tagged species since its approximate size is 30 kDa, and again this band was not observed in the empty vector or wild-type Pba1p pull down lanes. The proteins seen in the pull down lanes are the result of anti-flag elutions, so the detected proteins are present because they are either flag-tagged or associating with the flag-tagged protein, Pba1p-flag. Even though bands observed in the crosslinkable Pba1p pull down lane were promising, no protein was detected in the total fractions. I suspected this may be due to inefficient lysis, so I repeated the above experiment and changed the lysis method from spheroplasting to bead beating. Switching the lysis method did produce detectable amounts of protein in the total fractions (Figure 17). Additionally, potential α6-HA bands were detected at approximately 30 kDa in the Pba1p wild-type and crosslinkable pull down lanes; however, a crosslink was not detected via anti-HA immunoblot. Failure to detect a crosslink may be a consequence of the new lysis method. Bead beating allowed for detectable amounts of protein within the total lanes, but bead beating has been implicated in disrupting protein-protein interactions, potentially due to sample foaming and/or heating. So it is possible that the proteasomal intermediates within this lysate were damaged, due to the forces placed on the cells during the bead beating. This could potentially interfere with Pba1p interacting with the 20S CP. Another possibility for not detecting a crosslink in these strains could be due to the presence of

endogenous Pba1p. When the endogenous Pba1p interacts with the α5-α6 pocket, it will compete with the cys mutant for this pocket and thus decrease the likelihood of the engineered Pba1p interacting and subsequently crosslinking to the α5-α6 pocket. Fortunately, this can be overcome (see 4.7).

4.6 Conclusions

Despite several attempts, I was unable to detect the Pba1p-α6 or the Pba2p-α7 crosslinks. The lack of success with the first approach may be due to one or a combination of the following possibilities: the cysteines being too far apart for disulfide formation under mild oxidizing conditions, mutating the conserved lysine residue may have decreased the affinity of Pba1p-Pba2p to the 20S CP, and/or the endogenous cysteines found on α5 and α6 may have interfered with crosslinkable Pba1p and Pba2p crosslinking into their respective pockets.

After identifying these potential issues, an alternative crosslinking approach was undertaken using strains from another crosslinking study. This new yeast background contained the crosslinkable cysteine residues on the side of the α intersubunit pocket, allowing the conserved lysine residue to remain intact. To resolve any discrepancies involving the distance between the engineered cysteine residues, the crosslinking was performed using crosslinker BMOE; however, it bears mentioning that the Finley lab also succeeded in observing Rpt-α subunit crosslinks using $CuCl_2$ to induce cys-cys crosslinks, though the BMOE approach was likely more efficient (Tian et al, 2011). Additionally, the previously mentioned endogenous cysteine residues found on α5 and α6 were mutated

to alanines to prevent any non-specific crosslinking. All in all, this new strain of yeast should be able to crosslink with my cysteine HbYX mutant Pba1p and Pba2p proteins; however due to time constraints, I was only able to perform a few assays aiming to detect the Pba1p-α6 crosslink. Although these first few attempts were unsuccessful, I do believe that crosslinking can be achieved.

4.7 Future Work

On the whole, I believe that crosslinking is a feasible approach to identify the α intersubunit pockets to which Pba1p and Pba2p bind. Even though I plan to focus my attention on crosslinking Pba1p and Pba2p utilizing the Finley strains, the Pba2p-α7 results in the old approach, I believe, are worth further investigation (Figure 13B). Now that the detection issues are resolved, I would like to verify if the banding patterns observed in the Pba2p (WT) and α7 cysteine sample are in fact due to crosslinking. This can be done by both probing with anti-his and performing reducing controls on all of the samples.

Since the Finley strain α intersubunit pockets have been shown to successfully crosslink C-terminal HbYX motifs of Rpt subunits, the main focus for future work will involve crosslinking cysteine mutated Pba1p and Pba2p to the α intersubunit pockets in these strains. However, before the next crosslinking assays are conducted, I will delete the endogenous *PBA1* and *PBA2* genes in the Finley strain background. This will eliminate the possibility of endogenous Pba1p-Pba2p interfering with the plasmid-borne crosslinkable Pba1p and/or Pba2p binding to the 20S. Hopefully, with this additional

optimization I will be able to successfully crosslink Pba1p and Pba2p to their respective binding pockets.

TABLES

Table 1 Yeast Strains Used in This Study.

Name	Genotype
AKY600[1]	*MATa his3-Δ200 leu2-3,112 ura3-52 lys2-801 trp1-1 gal2*
AKY601[1]	*MATα his3-Δ200 leu2-3,112 ura3-52 lys2-801 trp1-1 gal2*
AKY612[2]	*MATa pre6Δ::HIS3* [pRS317 *pre6-N79C,I155C-His6]*
AKY613[2]	*MATa pre6Δ::HIS3 pre9Δ::HIS3* [pRS317 *pre6-N79C,I155C-His6]*
AKY607[3]	*MATα pba1Δ::kanMX*
AKY608[3]	*MATα pba2Δ::natMX*
AKY418[4]	*MATα rpn4Δ::hphMX*
AKY424[4]	*MATα rpn4Δ::hphMX pba1Δ::kanMX*
AKY425[4]	*MATα rpn4Δ::hphMX pba2Δ::natMX*
AKY615	*MATα pba1Δ::kanMX* [pRS314 *PBA1-Flag (TRP)*]
AKY616	*MATα pba1Δ::kanMX [pRS314 PBA1-I276C-Flag (TRP)]*
AKY647	*MATα pba2Δ::natMX* [pRS314 *PBA2-His6 (TRP)*]
AKY648	*MATα pba2Δ::natMX* [pRS314 *PBA2-N267C-His6 (TRP)*]
AKY634	*MATa his3Δ1 leu2Δ0 met15Δ0 ura3Δ0* [pRS314 *(TRP)*] [BG1805 *(URA)*]
AKY635	*MATα pba1Δ::kanMX* [pRS314 *PBA1-Flag (TRP)*] [BG1805 *PRE5-TAP (URA)*]
AKY636	*MATα pba1Δ::kanMX [pRS314 PBA1-Flag (TRP)] [BG1805 PRE5K66C-TAP (URA)]*
AKY637	*MATα pba1Δ::kanMX [pRS314 PBA1-I276C-Flag (TRP)] [BG1805 PRE5-TAP (URA)]*
AKY638	*MATα pba1Δ::kanMX [pRS314 PBA1-I275C-Flag (TRP)] [BG1805 PRE5-K66C-TAP (URA)]*
AKY673	*MATα pba2Δ::natMX* [pRS314 *PBA2-His6 (TRP)*][BG1805 *PRE10-TAP (URA)*]
AKY674	*MATα pba2Δ::natMX [pRS314 PBA2-His6 (TRP)][BG1805 PRE10-K66C-TAP (URA)]*
AKY675	*MATα pba2Δ::natMX [pRS314 PBA2-N267C-His6 (TRP)]* [*BG1805 PRE10-TAP (URA)*]
AKY676	*MATα pba2Δ::natMX* [*pRS314 PBA2-N267C-His6 (TRP)*][BG1805 PRE10-K66C-TAP (URA)]
AKY679[5]	*MATa scl1::scl1-I87C-6HA (HYG)*
AKY680[5]	*MATa pre8::pre8-G79C-6HA (HYG)*
AKY681[5]	*MATa pre9::pre9-T81C-6HA (HYG)*
AKY682[5]	*MATa pre6::pre6-N79C (URA)*
AKY683[5]	*MATa pup2::pup2-T82C-6HA (HYG) pre5::pre5-C113A (TRP)*
AKY684[5]	*MATa pre5::pre5-A78C-6HA (HYG) pre5::pre5-C113A (TRP)*
AKY685[5]	*MATa pre10-I82C-6HA (HYG) pre5::pre5-C113A (TRP)*
AKY689	*MATa pre5::pre5-A78C-6HA (HYG) pre5::pre5-C113A (TRP) [pRS316 (URA)]*
AKY690	*MATa pre5::pre5-A78C-6HA (HYG) pre5::pre5-C113A (TRP) [pRS316 PBA1-Flag (URA)]*
AKY691	*MATa pre5::pre5-A78C-6HA (HYG) pre5::pre5-C113A (TRP)* [pRS316 PBA1-I276C-Flag (URA)]
AKY702	*MATa his3-Δ200 leu2-3,112 ura3-52 lys2-801 trp1-1 gal2* [pRS316 *(URA)*]
AKY703	*MATa pre5::pre5-A78C-6HA (HYG) pre5::pre5-C113A (TRP)*[pRS316 *(URA)*]
AKY704	*MATa pre5::pre5-A78C-6HA (HYG) pre5::pre5-C113A (TRP)* [pRS316 PBA2-His6 *(URA)*]
AKY705	*MATa pre5::pre5-A78C-6HA (HYG) pre5::pre5-C113A (TRP)* [pRS316 *PBA2-N267C-His6 (URA)*]

AKB600 and AKB601 are wild-type strains and the remaining strains are congenic derivatives, except AKB634 whose background is BY4741.
All strains are from this study, except:
1. Chen and Hochstrasser (1995)
2. Verma et al. (2000)
3. Li et al. (2007)
4. Kusmierczyk et al. (2011)
5. Tian et al. (2011)

Table 2 Plasmids Used in This Study.

Name	Genotype
AKB490	pRS316 his-*PBA2*
AKB495	pRS316 flag-*PBA1*
AKB663	BG1803 *PRE9*-TAP
AKB665	BG1803 *PUP2*-TAP
AKB670	BG1805 SCL1-TAP
AKB671	BG1805 *PRE8*-TAP
AKB672	BG1805 *PRE6*-TAP
AKB673	BG1805 *PRE5*-TAP
AKB674	BG1805 *PRE10*-TAP
AKB675	BG1805 *scl1*(KY71C)-TAP
AKB676	BG1805 *pre8*(K64C)-TAP
AKB677	BG1805 *pre9*(K65C)-TAP
AKB678	BG1805 *pre6*(K63C)-TAP
AKB679	BG1805 *pup2*(K66C)-TAP
AKB680	BG1805 *pre5*(K62C)-TAP
AKB681	BG1805 *pre10*(K66C)-TAP
AKB684	pRS316 flag-*pba1*(I276C)
AKB685	pRS316 his-*pba2*(N267C)
AKB692	pRS314 flag-*PBA1*
AKB693	pRS314 flag-*pba1*(I276C)
AKB694	pRS314 his-*PBA2*
AKB695	pRS314 his-*pba2*(N267C)

Table 3 Antibody Dilutions Used in This Study.

Antibody	Dilution
Anti-Hemaglutinin (Anti-HA)	1:1000
Peroxidase Anti-Peroxidase (Anti-PAP)	1:10000
Anti-Tetra-His	1:1000
Anti-Flag	1:1000
Goat Anti-Mouse	1:5000

FIGURES

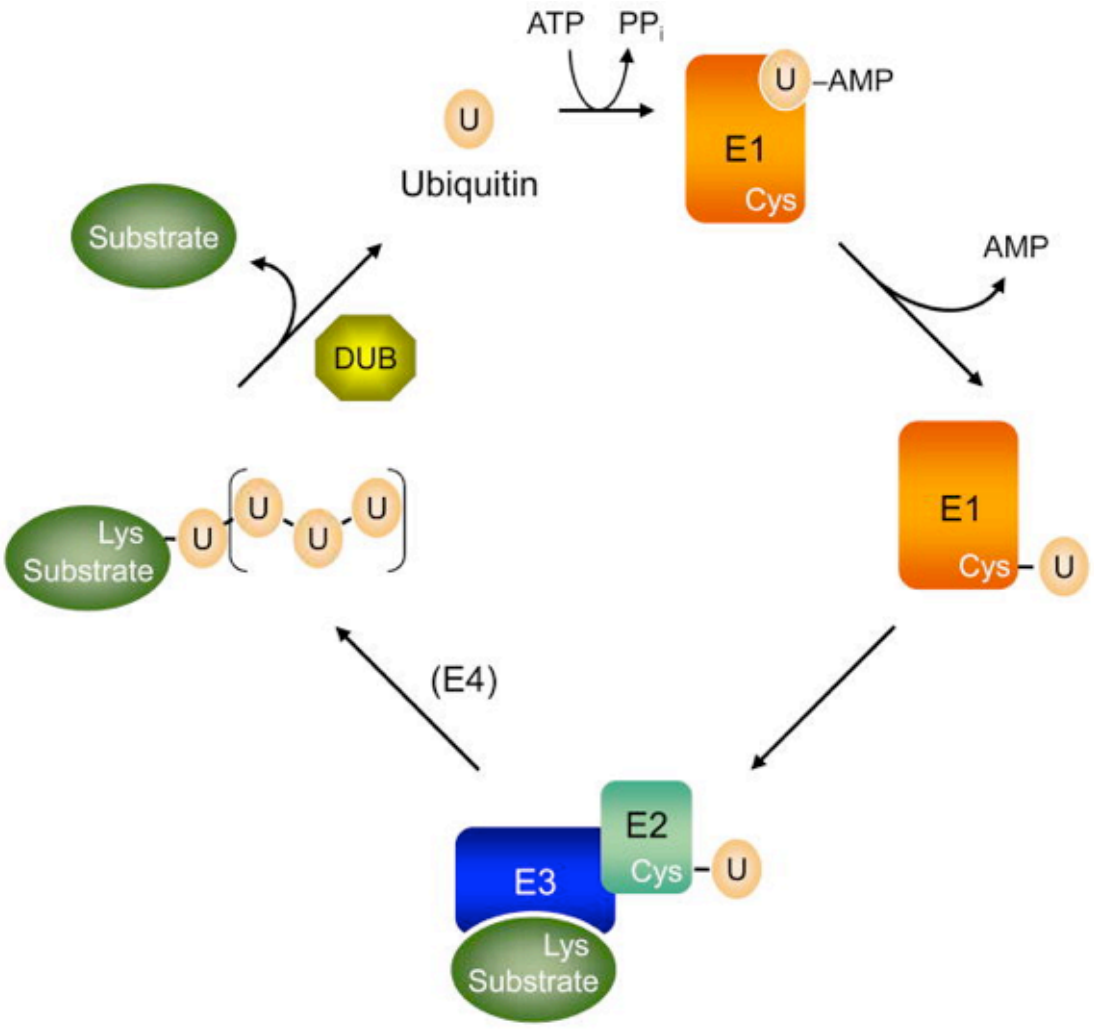

Figure 1 Schematic of Ubiquitination
A schematic of a protein being modified by ubiquitin. The process of ubiquitination is an ATP dependent process that is carried out by three different enzymes E1, E2, and E3. E1 is responsible for activating the C-terminal glycine residue of ubiquitin so that it may form a covalent bond with the lysine of the target protein. E2 and E3 aid in the attachment of the activated ubiquitin to a substrate. Once a substrate has been ubiquitinated, that attached ubiquitin may under go several rounds of ubiquitination forming a ubiquitin chain. The additional ubiquitin proteins are attached via E4. Attached ubiquitin proteins are removed from the substrate by DUB (deubiquitinating enzymes) (Hochstrasser, 2009).

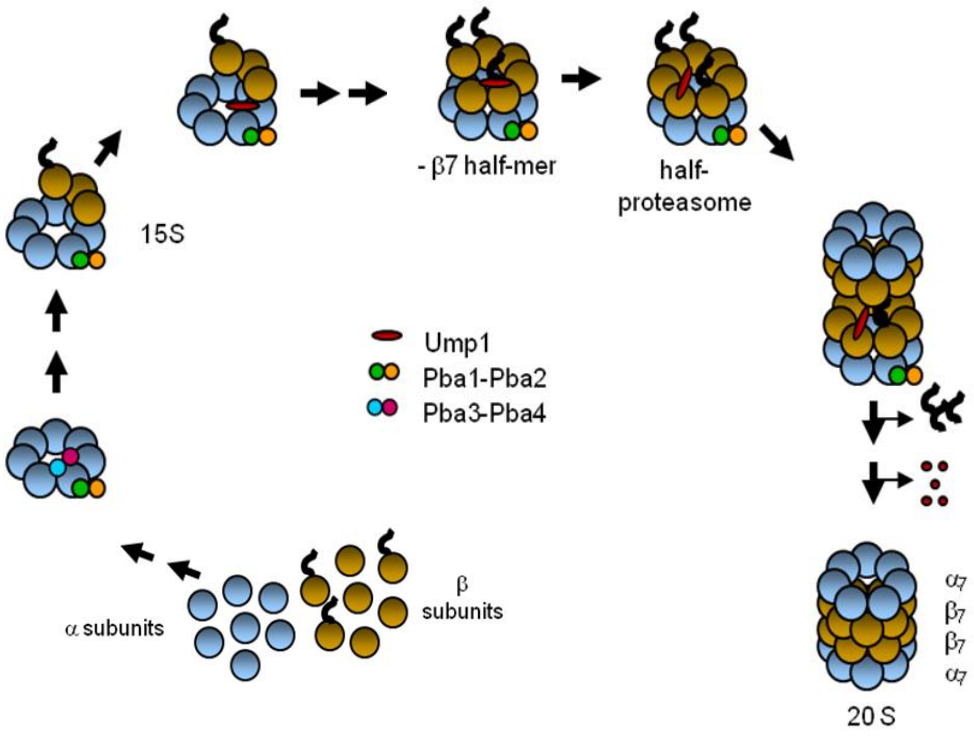

Figure 2 20S Assembly

The current picture of 20S assembly begins with free α and β subunits (bottom left). The dark squiggly line on three of the β subunits corresponds to the propeptides found on β1, β2, and β5. The first step in assembly involves the formation of an α-ring. This α-ring acts a scaffold for β subunits to assemble onto. The earliest proteasome intermediate that has been isolated in yeast is the 15S, which consists of one full α-ring and three β subunits. Once all of the seven β subunits assemble to an α-ring, this structure is referred to as the 'half-proteasome.' To complete assembly, two half-proteasomes will dimerize. Once dimerization has occurred the propeptides are cleaved, resulting in the 20S proteasome. The proteins listed in the center of the figure correspond to known chaperone proteins involved in 20S assembly (see above 1.7 Chaperone Proteins).

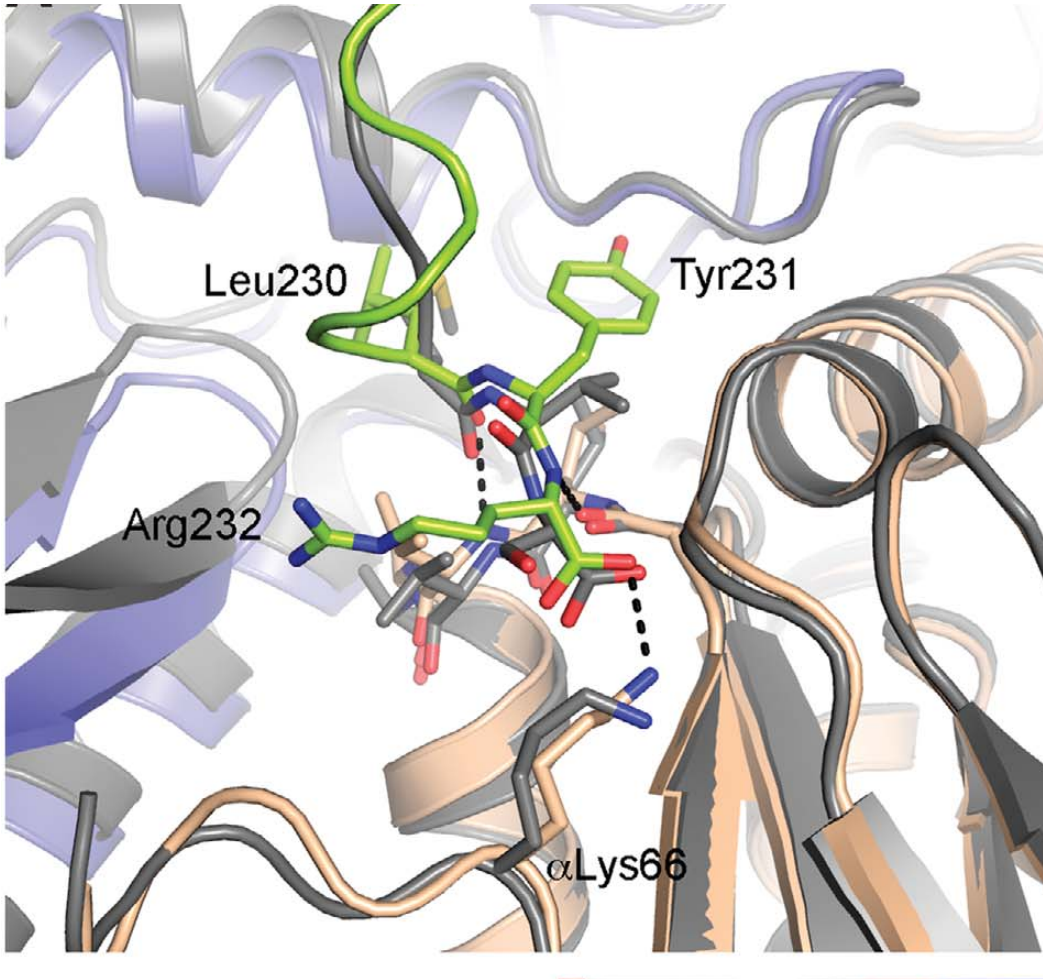

Figure 3 α-intersubunit Binding
Activator HbYX motifs have been shown to interact with α intersubunit pockets. This figure compares the interaction of PA26 (grey) and PAN (green) C-termini binding to the α intersubunit pocket. PAN contains a C-terminal HbYX motif while PA26 does not (Yu et al, 2010).

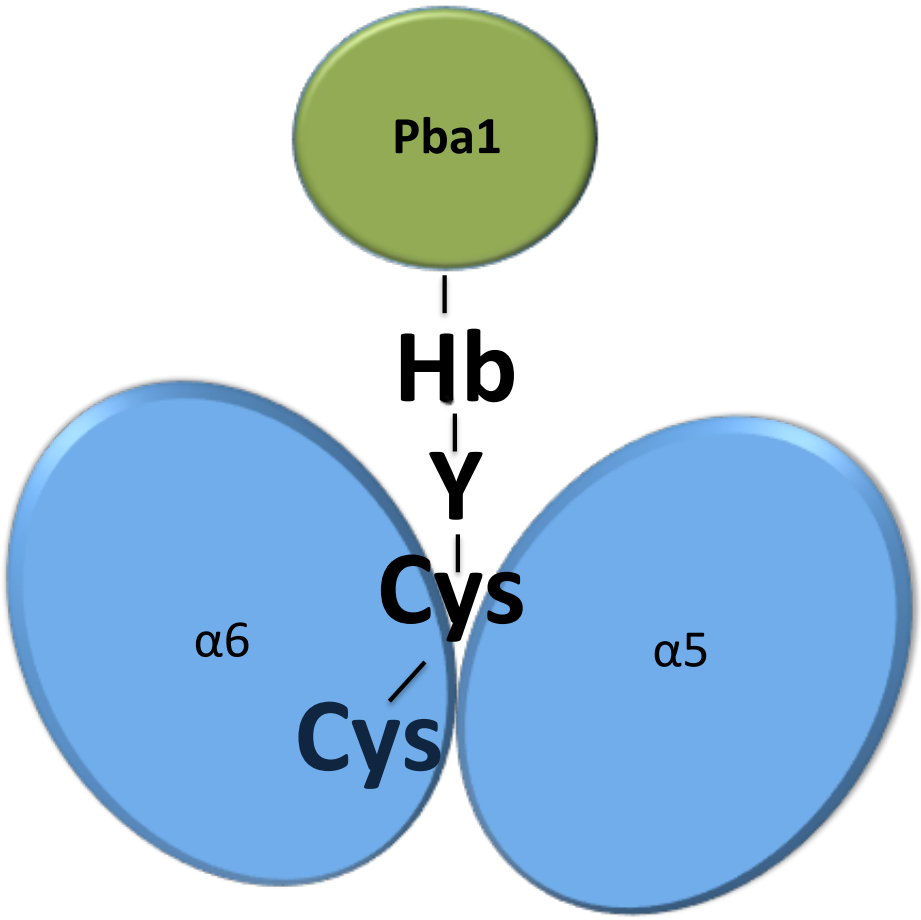

Figure 4 Crosslinking Strategy
Schematic of the $CuCl_2$ induced crosslinking strategy. The depicted interaction should occur only when the correct combination of crosslinkable Pba1p (or Pba2p) and crosslinkable α subunit are exposed to mild oxidizing conditions.

```
a1   61 DKLLDP-TTVSYIFCISRTIGMVVNGPIPDARNAALRAKAEAAE-FRYKYGYDMPCDVLA
a2   53 SPLAMSET-LSKVSLLTPDIGAVYSGMGPDYRVLVDKSRKVAHTSYKRIYGEYPPTKLLV
a3   54 STLLEQDTSTEKLYKLNDKIAVAVAGLTADAEILINTARIHAQN-YLKTYNEDIPVEILV
a4   52 LKLQDTRITPSKVSKIDSHVVLSFSGLNADSRILIEKARVEAQS-HRLTLEDPVTVEYLT
a5   56 SPLLES-DSIEKIVEIDRHIGCAMSGLTADARSMIEHARTAAVT-HNLYYDEDINVESLT
a6   54 DELSS---YQKKIIKCDEHMGLSLAGLAPDARVLSNYLRQQCNY-SSLVFNRKLAVERAG
a7   56 SKLLVP-QKNVKIQVVDRHIGCVYSGLIPDGRHLVNRGREEAAS-FKKLYKTPIPIPAFA
```

Figure 5 α-subunit Sequence Alignment

Yeast α subunit sequence alignment. The conserved K66 position (using numbering from the archaeon *T. acidophilum*) is indicated in red. The only subunit lacking the conserved lysine residue is α1, which has tyrosine residue at that position.

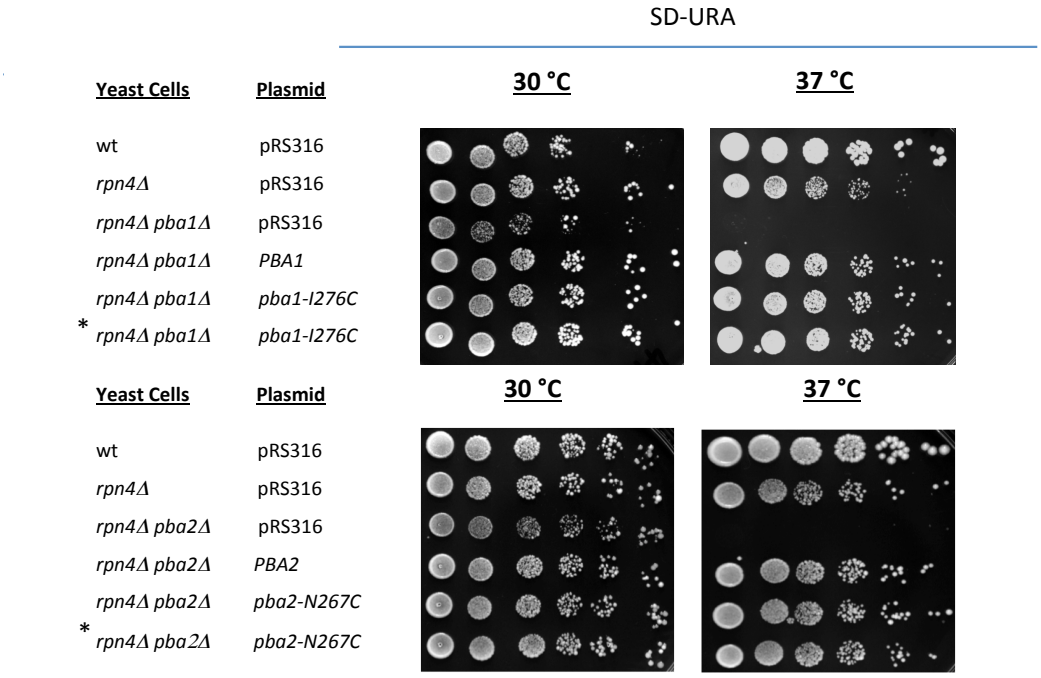

Figure 6 Dilution Series *pba1-C pba2-C*
The Pba1p and Pba2p HbYX (X →C) mutations do not affect the growth of the yeast. Yeast strains were transformed with an empty vector or with a vector containing the indicated *PBA* constructs. A six-fold dilution series of liquid yeast cultures were spotted on to SD-Ura media and incubated at 30 °C and 37 °C. The HbYX mutant constructs were transformed in duplicate (*).

A

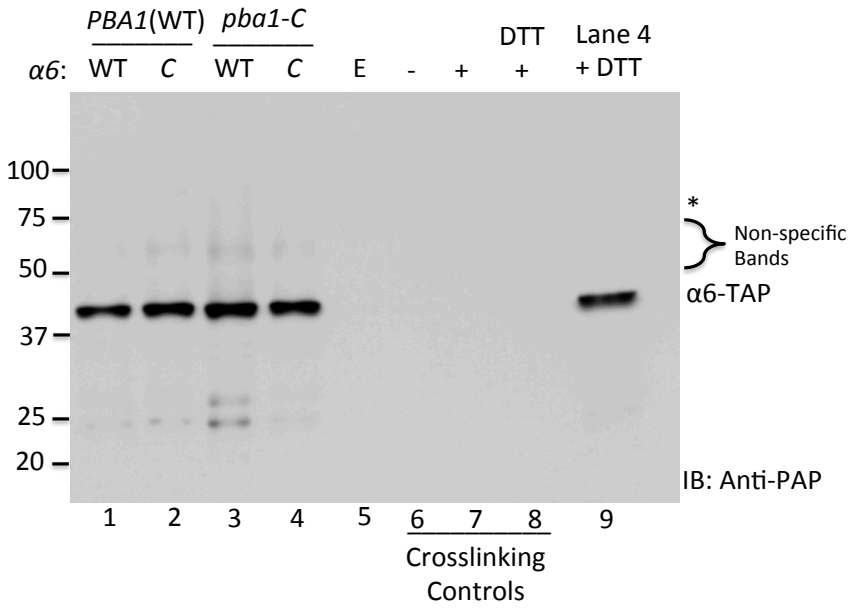

Figure 7 A Pba1p-α6 $CuCl_2$ Crosslinking

Yeast strains were generated to contain either wild-type (WT) Pba1p and α6 or both Pba1p and α6 engineered with cysteine residues (C). These cysteines will come within close proximity of one another if the α5-α6 pocket is the correct binding site for Pba1p. Disulfide crosslinking was induced by incubating whole cell lysate from 5 ml cultures in 0.25 mM $CuCl_2$ for 60 minutes. Following crosslinking, samples were electrophoresed on 10% non-reducing SDS-PAGE and transferred to PVDF membrane. Crosslinking was visualized by anti-PAP immunoblotting. The Pba1-α6 crosslink should be observed in lane 4 at approximately 75 kDa (position denoted with *); however, no such band was detected. Lanes 6, 7, and 8 are the crosslinking controls. These samples were visualized with Anti-Tetra-His antibody (Figure 7B). Strains used were AKY635 (lane1), AKY636 (lane 2), AKY637 (lane 3), AKY638 (lanes 4 and 9), AKY634 (lane 5), AKY612, and AKY613 (lanes 7 and 8). Reducing agent was added where indicated prior to loading the gel. Lanes 6-8 represent positive control samples, described in (B). E denotes wild-type yeast strain transformed with empty vectors.

B

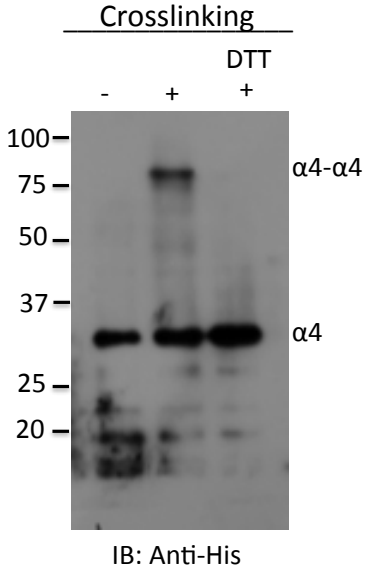

Figure 7 B Pba1p-α6 $CuCl_2$ Crosslinking Controls
Crosslinking controls for Pba1p and α6 crosslinking (5 ml). The control strains contain α4 subunits with engineered cysteines that will come into close proximity if two α4 subunits are positioned next to each other within an α-ring. Previous work has demonstrated that this will occur when α3 is deleted (Velichutina et al, 2004). For this control assay all lanes contained crosslinkable α4 and all lanes were treated with $CuCl_2$. However, crosslinking occurred only in the strains where α3 is deleted (+) and not in strains where α3 is still present (-). The crosslinked α4-α4 species is indicated, as is the α4 monomer. Reducing agent DTT was added where indicated prior to loading the gel.

A

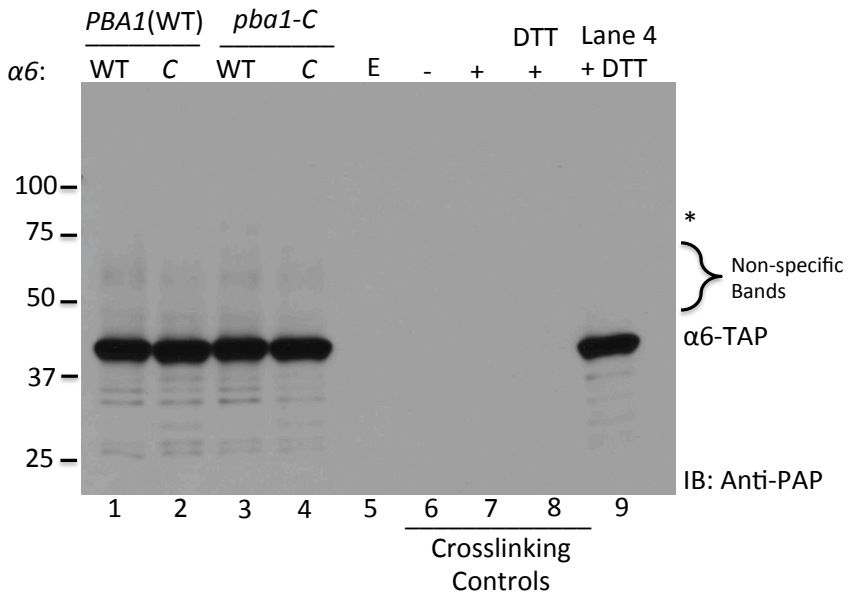

Figure 8 A Pba1p-α6 $CuCl_2$ Crosslinking 2-Fold Increase in Protein Concentration
Yeast strains were generated to contain either wild-type (WT) Pba1p and α6 or both Pba1p and α6 engineered with cysteine residues (C). These cysteines will come within close proximity of one another if the α5-α6 pocket is the correct binding site for Pba1p. Disulfide crosslinking was induced by incubating whole cell lysate from 10 ml cultures in 0.25 mM $CuCl_2$ for 60 minutes. Following crosslinking, samples were electrophoresed on 10% non-reducing SDS-PAGE and transferred to PVDF membrane. Crosslinking was visualized by anti-PAP immunoblotting. The Pba1-α6 crosslink was expected in lane 4 at approximately 75 kDa (position denoted with *); however, no such band was detected. Lanes 6, 7, and 8 are the crosslinking controls. These samples were visualized with Anti-Tetra-His antibody (Figure 8B). Strains used were AKY635 (lane1), AKY636 (lane 2), AKY637 (lane 3), AKY638 (lanes 4 and 9), AKY634 (lane 5), AKY612, and AKY613 (lanes 7 and 8). Reducing agent was added where indicated prior to loading the gel. Lanes 6-8 represent positive control samples, described in (B). E denotes wild-type yeast strain transformed with empty vectors

B

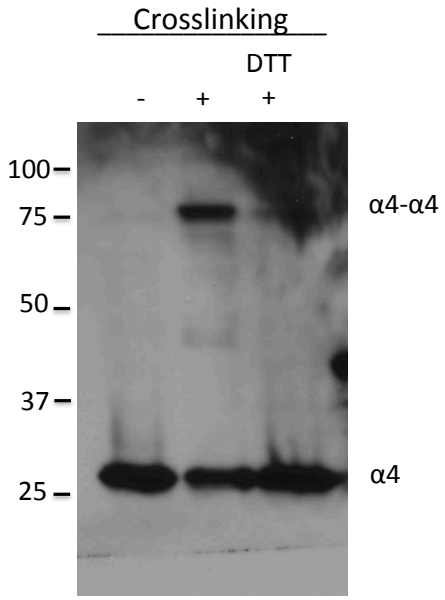

Figure 8 B Crosslinking Controls: Pba1p-α6 $CuCl_2$ Crosslinking 2-Fold Increase in Protein Concentration

Crosslinking controls for Pba1p and α6 crosslinking (10 ml). The control strains contain α4 subunits with engineered cysteines that will come into close proximity if two α4 subunits are positioned next to each other within a α-ring. Previous work has demonstrated that this will occur when α3 is deleted (Velichutina et al, 2004). For this control assay all lanes contained crosslinkable α4 and all lanes were treated with $CuCl_2$. However, crosslinking occurred only in the strains where α3 is deleted (+) and not in strains where α3 is still present (-). The crosslinked α4-α4 species is indicated, as is the α4 monomer. Reducing agent DTT was added where indicated prior to loading the gel.

A

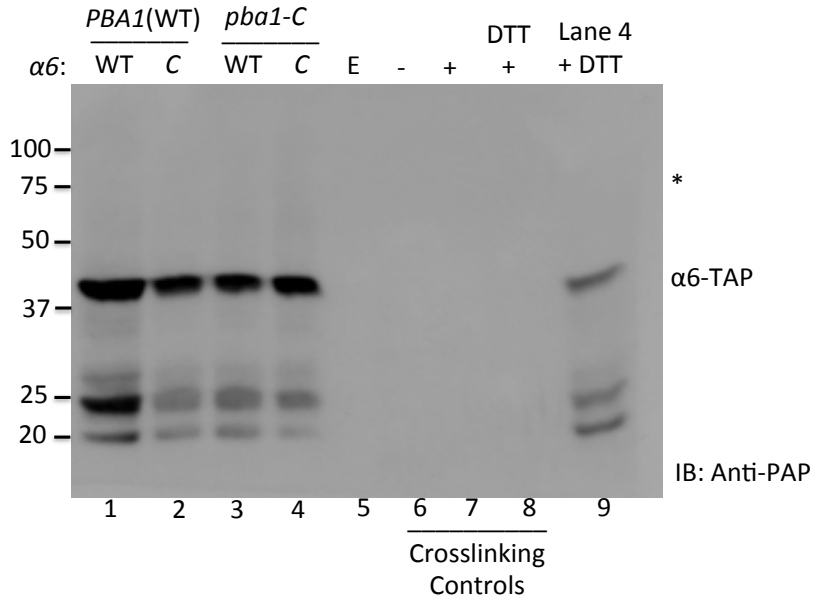

Figure 9 A Pba1p-α6 $CuCl_2$ Crosslinking 10-Fold Increase in Protein Concentration Yeast strains were generated to contain either wild-type (WT) Pba1p and α6 or both Pba1p and α6 engineered with cysteine residues (C). These cysteines will come within close proximity of one another if the α5-α6 pocket is the correct binding site for Pba1p. The crosslink is predicted to run at approximately 75 kDa (position denoted by *). Disulfide crosslinking was induced by incubating whole cell lysate from 50 ml cultures in 0.25 mM $CuCl_2$ for 60 minutes. Following crosslinking, samples were electrophoresed on 10% non-reducing SDS-PAGE and transferred to PVDF membrane. Crosslinking was visualized by anti-PAP immunoblotting. The Pba1-α6 crosslink was expected in lane 4 at approximately 75 kDa (position denoted with *); however, no such band was detected. Lanes 6, 7, and 8 are the crosslinking controls. These samples were visualized with Anti-Tetra-His antibody (Figure 9B). Strains used were AKY635 (lane1), AKY636 (lane 2), AKY637 (lane 3), AKY638 (lanes 4 and 9), AKY634 (lane 5), AKY612, and AKY613 (lanes 7 and 8). Reducing agent was added where indicated prior to loading the gel. Lanes 6-8 represent positive control samples, described in (B). E denotes wild-type yeast strain transformed with empty vectors.

B

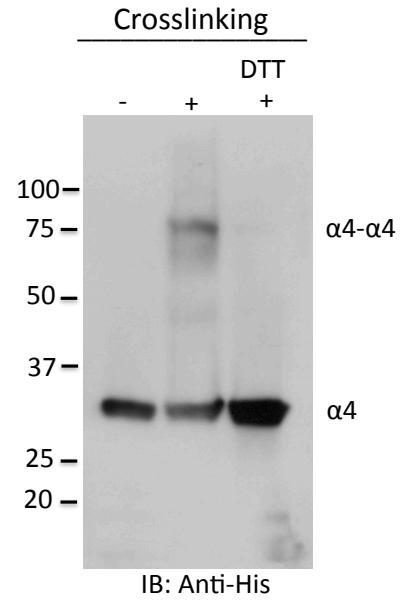

Figure 9 B Crosslinking Controls: Pba1p-α6 $CuCl_2$ Crosslinking 10-Fold Increase in Protein Concentration

Crosslinking controls for Pba1p and α6 crosslinking (50 ml). The control strains contain α4 subunits with engineered cysteines that will come into close proximity if two α4 subunits are positioned next to each other within a α-ring. Previous work has demonstrated that this will occur when α3 is deleted (Velichutina et al, 2004). For this control assay all lanes contained crosslinkable α4 and all lanes were treated with $CuCl_2$. However, crosslinking occurred only in the strains where α3 is deleted (+) and not in strains where α3 is still present (-). The crosslinked α4-α4 species is indicated, as is the α4 monomer. Reducing agent DTT was added where indicated prior to loading the gel.

A

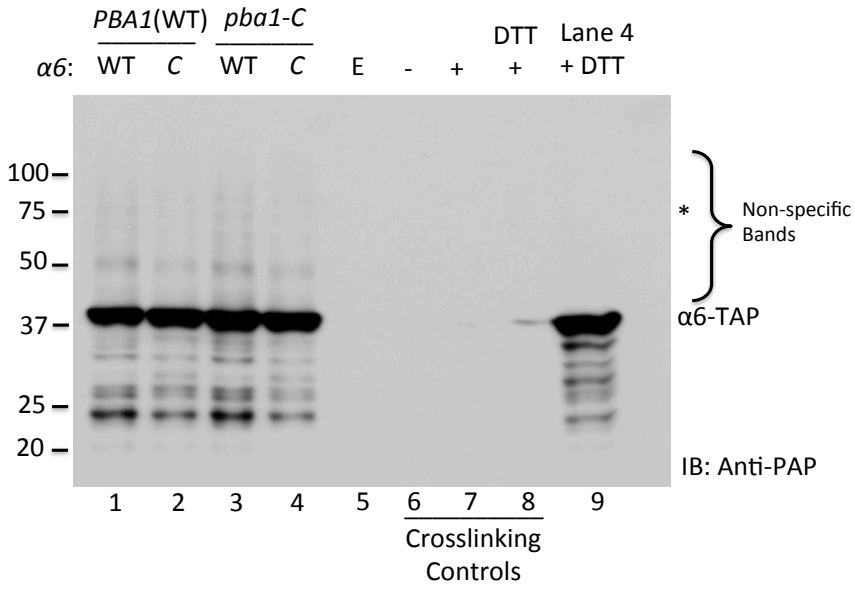

Figure 10 A Pba1p-α6 $CuCl_2$ Crosslinking 10-Fold Increase in Protein Concentration + MG132

Yeast strains were generated to contain either wild-type (WT) Pba1p and α6 or both Pba1p and α6 engineered with cysteine residues (C). These cysteines will come within close proximity of one another if the α5-α6 pocket is the correct binding site for Pba1p. In an attempt to increase the binding affinity, the lysate was incubated in 20 μM MG132 prior to crosslinking. Disulfide crosslinking was induced by incubating whole cell lysate from 50 ml cultures in 0.25 mM $CuCl_2$ for 60 minutes. Following crosslinking, samples were electrophoresed on 10% non-reducing SDS-PAGE and transferred to PVDF membrane. Crosslinking was visualized by anti-PAP immunoblotting. The Pba1-α6 crosslink was expected in lane 4 at approximately 75 kDa (position denoted with *); however, no such band was detected. Lanes 6, 7, and 8 are the crosslinking controls. These samples were visualized with Anti-Tetra-His antibody (Figure 10B). Strains used were AKY635 (lane1), AKY636 (lane 2), AKY637 (lane 3), AKY638 (lanes 4 and 9), AKY634 (lane 5), AKY612, and AKY613 (lanes 7 and 8). Reducing agent was added where indicated prior to loading the gel. Lanes 6-8 represent positive control samples, described in (B). E denotes wild-type yeast strain transformed with empty vectors.

B

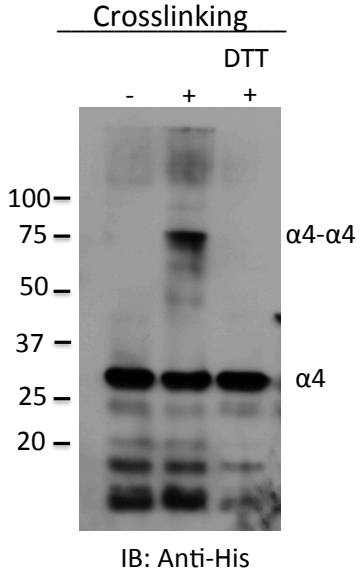

Figure 10 B Crosslinking Controls: Pba1p-α6 $CuCl_2$ Crosslinking 10-Fold Increase in Protein Concentration + MG132

Crosslinking controls for Pba1p and α6 crosslinking (50 ml + MG132). The control strains contain α4 subunits with engineered cysteines that will come into close proximity if two α4 subunits are positioned next to each other within a α-ring. Previous work has demonstrated that this will occur when α3 is deleted (Velichutina et al, 2004). For this control assay all lanes contained crosslinkable α4 and all lanes were treated with $CuCl_2$. However, crosslinking occurred only in the strains where α3 is deleted (+) and not in strains where α3 is still present (-). The crosslinked α4-α4 species is indicated, as is the α4 monomer. Reducing agent DTT was added where indicated prior to loading the gel.

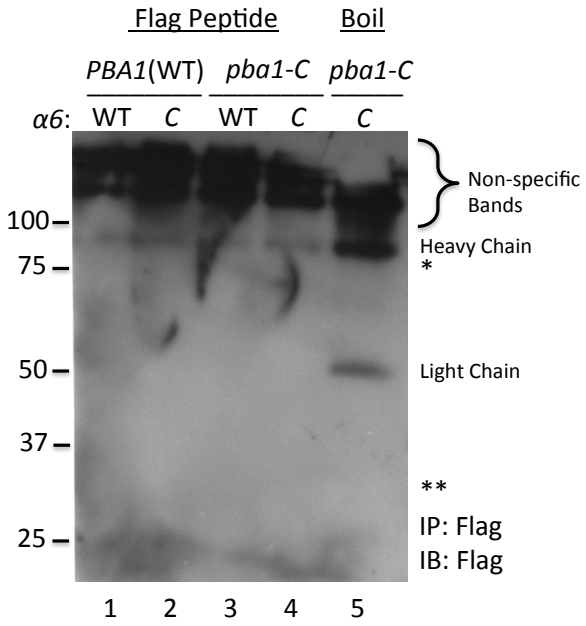

Figure 11 Pba1p-α6 $CuCl_2$ Crosslinking 10-Fold Increase in Protein Concentration + MG132 + Flag Pull-Down

Yeast strains were generated to contain either wild-type (WT) Pba1p and α6 or Pba1p and α6 engineered with cysteine residues (C). These cysteines will come within close proximity of one another if the α5-α6 pocket is the correct binding site for Pba1p. In an attempt to increase the binding affinity, the lysate was incubated in 20 μM MG132 prior to crosslinking. Disulfide crosslinking was induced by incubating whole cell lysate from 50 ml cultures in 0.25 mM $CuCl_2$ for 60 minutes. Following crosslinking, samples were immunoprecipitated with M2 Flag resin. The elutions were carried out as indicated, and the eluates were electrophoresed on 10% non-reducing SDS-PAGE then transferred to PVDF membrane. Crosslinking was visualized by anti-PAP immunoblotting. The Pba1-α6 crosslink was expected in lanes 4 and 5 at approximately 75 kDa (position denoted with *); however, no such band was detected. Additionally, the Pba1-Flag species should have been observed in all lanes (position denoted with **), but the band corresponding to this protein was not detected. Strains used were AKY635 (lane1), AKY636 (lane 2), AKY637 (lane 3), AKY638 (lanes 4 and 5).

A

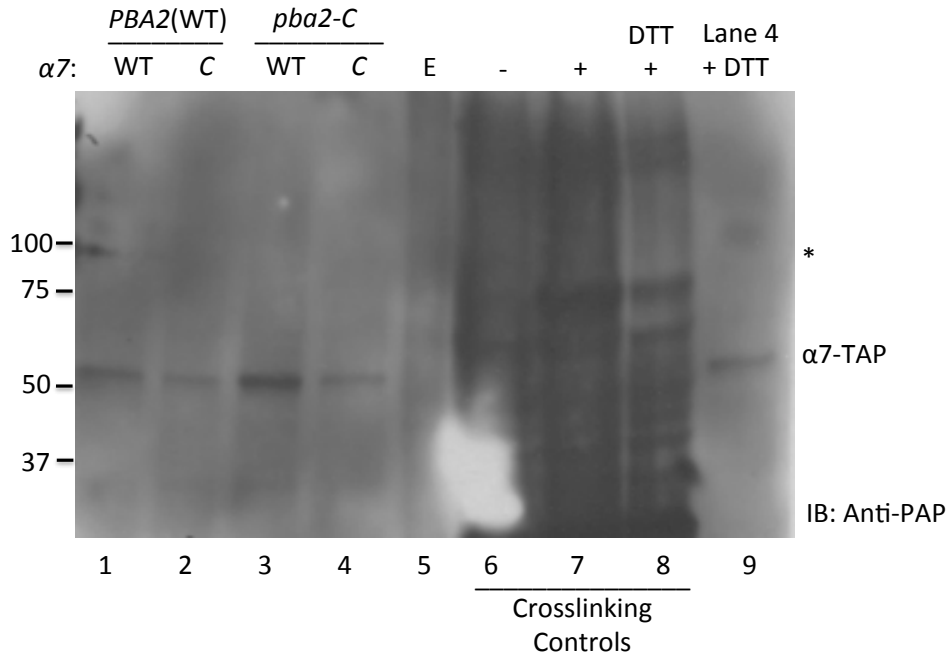

Figure 12 A Pba2p-α7 $CuCl_2$ Crosslinking
Yeast strains were generated to contain either wild-type (WT) Pba2p and α7 or both Pba2p and α7 engineered with cysteine residues (C). These cysteines will come within close proximity of one another if the α6-α7 pocket is the correct binding site for Pba2p. Disulfide crosslinking was induced by incubating whole cell lysate from 5 ml cultures in 0.25 mM $CuCl_2$ for 60 minutes. Following crosslinking, samples were electrophoresed on 10% non-reducing SDS-PAGE and transferred to PVDF membrane. Crosslinking was visualized by anti-PAP immunoblotting. The Pba2-α7 crosslink should be observed in lane 4 at approximately 80 kDa (position denoted with *); however, no such band was detected. Lanes 6, 7, and 8 are the crosslinking controls. These samples were visualized with Anti-Tetra-His antibody (Figure 12B). Strains used were AKY673 (lane1), AKY674 (lane 2), AKY675 (lane 3), AKY676 (lanes 4 and 9), AKY634 (lane 5), AKY612 (lane 6), and AKY613 (lanes 7 and 8). Reducing agent was added where indicated prior to loading the gel. Lanes 6-8 represent positive control samples, described in (B). E denotes wild-type yeast strain transformed with empty vectors.

B

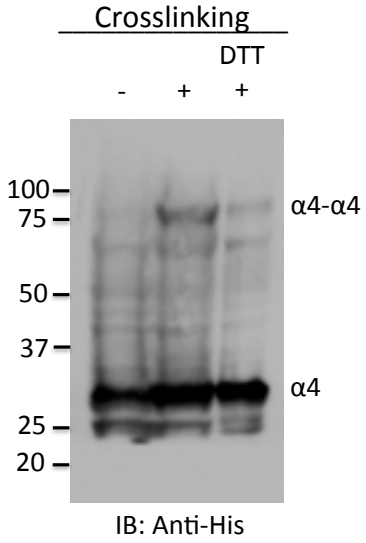

Figure 12 B Pba2p-α7 $CuCl_2$ Crosslinking Controls
Crosslinking controls for Pba2p and α7 crosslinking (5 ml). The control strains contain α4 subunits with engineered cysteines that will come into close proximity if two α4 subunits are positioned next to each other within a α-ring. Previous work has demonstrated that this will occur when α3 is deleted (Velichutina et al, 2004). For this control assay all lanes contained crosslinkable α4 and all lanes were treated with $CuCl_2$. However, crosslinking occurred only in the strains where α3 is deleted (+) and not in strains where α3 is still present (-). The crosslinked α4-α4 species is indicated, as is the α4 monomer. Reducing agent DTT was added where indicated prior to loading the gel.

A

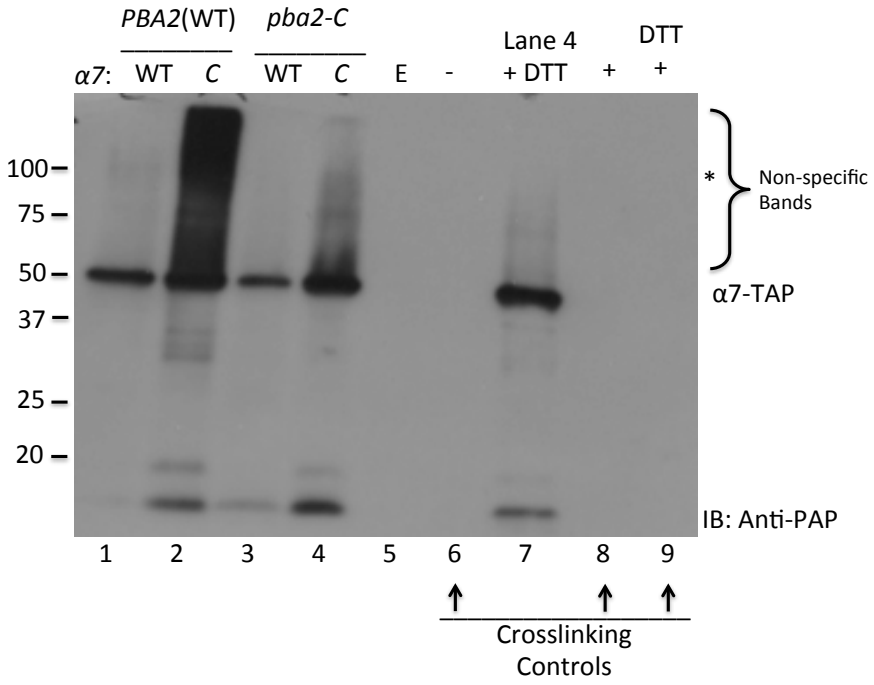

Figure 13 A Pba2p-α7 $CuCl_2$ Crosslinking 10-Fold Increase in Protein Concentration Yeast strains were generated to contain either wild-type (WT) Pba2p and α7 or Pba2p and α7 engineered with cysteine residues (C). These cysteines will come within close proximity of one another if the α6-α7 pocket is the correct binding site for Pba2p. Disulfide crosslinking was induced by incubating whole cell lysate from 50 ml cultures in 0.25 mM $CuCl_2$ for 60 minutes. Following crosslinking, samples were electrophoresed on 10 % non-reducing SDS-PAGE and transferred to PVDF membrane. Crosslinking was visualized by anti-PAP immunoblotting. The Pba2-α7 crosslink should be observed in lane 4 at approximately 80 kDa (position denoted with *); however, no such band was detected. Lanes 6, 8, and 9 are the crosslinking controls. These samples were visualized with Anti-Tetra-His antibody (Figure 13B). Strains used were AKY673 (lane1), AKY674 (lane 2), AKY675 (lane 3), AKY676 (lanes 4 and 7), AKY634 (lane 5), AKY612 (lane 6), and AKY613 (lanes 7, 8, and 9). Reducing agent was added where indicated prior to loading the gel. Lanes 6-8 represent positive control samples, described in (B). E denotes wild-type yeast strain transformed with empty vectors.

B

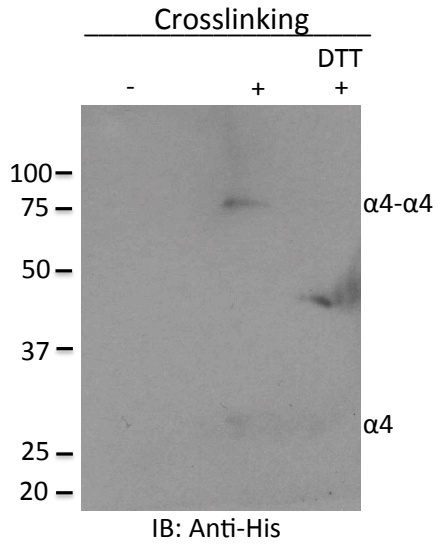

Figure 13 A Crosslinking Controls: Pba2p-α7 $CuCl_2$ Crosslinking 10-Fold Increase in Protein Concentration

Crosslinking control for Pba2p and α7 crosslinking (50 ml). The control strains contain α4 subunits with engineered cysteines that will come into close proximity if two α4 subunits are positioned next to each other within a α-ring. Previous work has demonstrated that this will occur when α3 is deleted (Velichutina et al, 2004). For this control assay all lanes contained crosslinkable α4, and all lanes were treated with $CuCl_2$. To better visualize the assay contrast and brightness levels were adjusted. The inability to clearly detect the α4 monomer suggests that the problem with this assay is not necessarily crosslinking, but a detection issue. Reducing agent DTT was added where indicated prior to loading the gel.

A

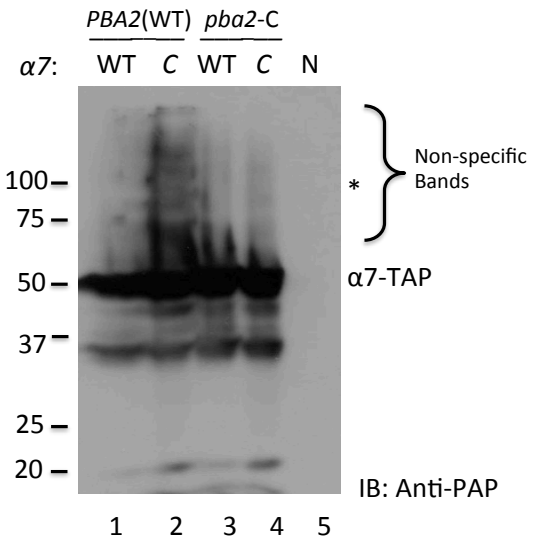

Figure 14 A Total Fractions of Pba2p-α7 $CuCl_2$ Crosslinking with a 10-Fold Increase in Protein Concentration + MG132 + Ni-NTA Pull-Down

Yeast strains were generated to contain either wild-type (WT) Pba2p and α7 or Pba2p and α7 engineered with cysteine residues (C). These cysteines will come within close proximity of one another if the α6-α7 pocket is the correct binding site for Pba2p. Prior to crosslinking, the lysate was incubated in 20 µM MG132. Disulfide crosslinking was induced by incubating whole cell lysate from 50 ml cultures in 0.25 mM $CuCl_2$ for 60 minutes. Lysates were run on a Ni NTA column. Total fractions (15 µl of the 100 µl lysate) were electrophoresed on 10 % non-reducing SDS-PAGE and transferred to PVDF membrane. The samples were visualized by anti-PAP immunoblotting. The Pba2-α7 crosslink should be observed in lane 4 at approximately 80 kDa (position denoted with *); however, no such band was detected. Strains used were AKY673 (lane 1), AKY674 (lane 2), AKY675 (lane 3), AKY676 (lanes 4), and AKY600 (lane 5). N denotes wild-type yeast strain without vectors.

B

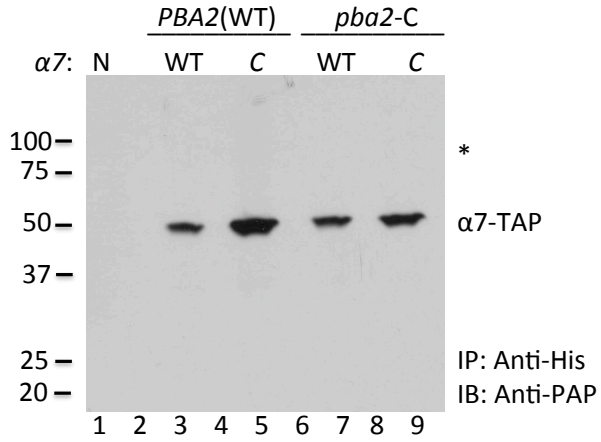

Figure 14 B Elute Fractions of Pba2p-α7 $CuCl_2$ Crosslinking with a 10-Fold Increase in Protein Concentration + MG132 + Ni-NTA Pull-Down

Pba2p and α7 were each engineered with cysteine residues. These cysteines will come within close proximity of one another if the α7-α6 pocket is the correct binding site for Pba2p. Prior to crosslinking the lysate obtained from the 50 ml cultures was incubated in proteasome inhibitor MG132. Disulfide crosslinking was induced by incubating whole cell lysate in $CuCl_2$ for 60 minutes. Lysates were applied to a Ni NTA column and eluted with imidazole-containing buffer as described in the materials and methods. Samples of the eluates were applied to non-reducing 10 % SDS-PAGE and blotted to PVDF prior to immunoblot analysis with anti-PAP. The Pba2-α7 crosslink should be observed in lane 9 at approximately 80 kDa (position denoted with *); however, no such band was detected. N denotes wild-type yeast strain without vectors.

C

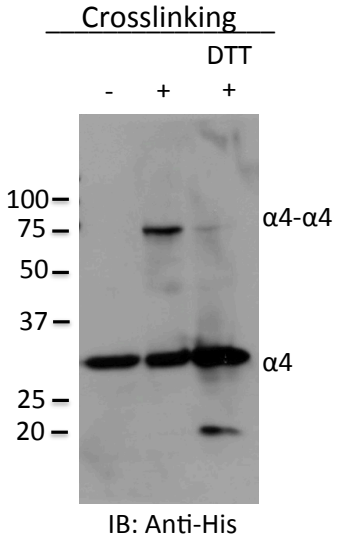

Figure 14 C Crosslinking Controls: Pba2p-α7 $CuCl_2$ Crosslinking with a 10-Fold Increase in Protein Concentration + MG132 + Ni-NTA Pull-Down

Crosslinking control for Pba2p and α7 crosslinking (50 ml + MG132). The control strains contain α4 subunits with engineered cysteines that will come into close proximity if two α4 subunits are positioned next to each other within a α-ring. Previous work has demonstrated that this will occur when α3 is deleted (Velichutina et al, 2004). For this control assay all lanes contained crosslinkable α4 and all lanes were treated with $CuCl_2$. However, crosslinking occurred only in the strains where α3 is deleted (+) and not in strains where α3 is still present (-). The crosslinked α4-α4 species is indicated, as is the α4 monomer. Reducing agent DTT was added where indicated prior to loading the gel.

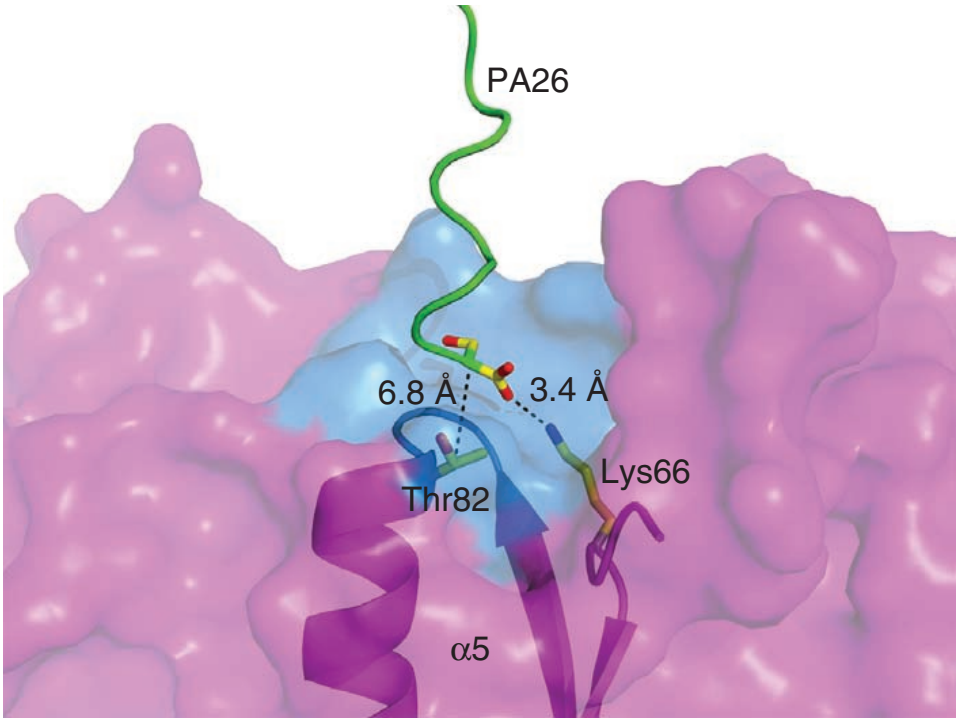

Figure 15 Representation of Finley Crosslinking Strategy
Representation of the Finley crosslinking strategy. The α4-α5 (blue) intersubunit pocket is depicted along with the C-terminus of a PA26 subunit. In order to crosslink C-termini into the intersubunit pockets specific residues were mutagenized to cysteines. A non-conserved residue on the side of the pocket, Thr82 residue on α5, was mutagenized to a cysteine. The distances between the C-terminus of PA26 and Thr82, as well as Lys66 are indicated (Tian et al, 2011).

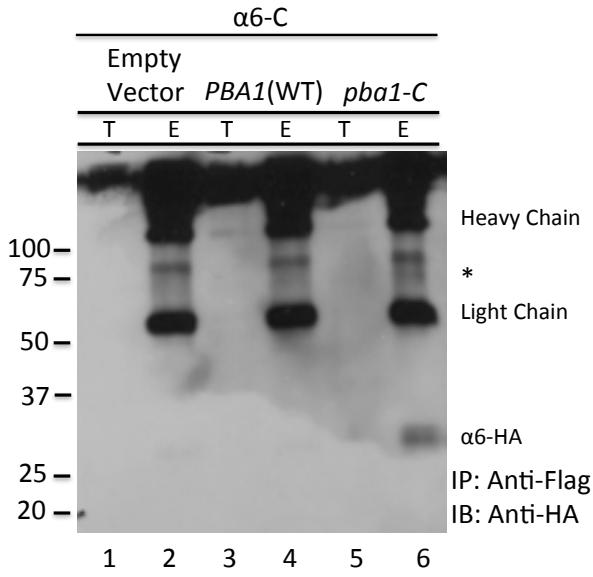

Figure 16 Pba1p-α6 BMOE Crosslinking Under Non-Reducing Conditions + MG132 + Flag Pull-Down

Pba1p and α6 were each engineered with cysteine residues (C). These cysteines will come within close proximity of one another if the α5-α6 pocket is the correct binding site for Pba1p. Prior to crosslinking, the samples were incubated in proteasome inhibitor MG132. Disulfide crosslinking was induced by incubating whole cell lysate from 50 ml cultures in BMOE for 60 minutes. Total fractions (20 µl) of the lysate were collected (T), and the remaining lysate was incubated in M2 Flag resin. The flag-tagged Pba1 proteins were eluted by boiling the resin in 20 µl sample buffer (E). After non-reducing SDS-PAGE (10%), the crosslinking was visualized by anti-HA immunoblotting. Within the eluate lane containing crosslinkable Pba1p (lane 6), there are two specific bands. One band is present at approximately 30 kDa corresponding to the α6-HA species (lane 6). The second band is located at approximately 60 kDa (*) corresponding to the size of a Pba1p-α6 crosslink (lane 6). These bands are not detected in the wild-type or empty vector eluate lanes (2 and 4). Strains used were AKY689 (lanes 1 and 2), AKY690 (lane 3 and 4), AKY691 (lane 5 and 6).

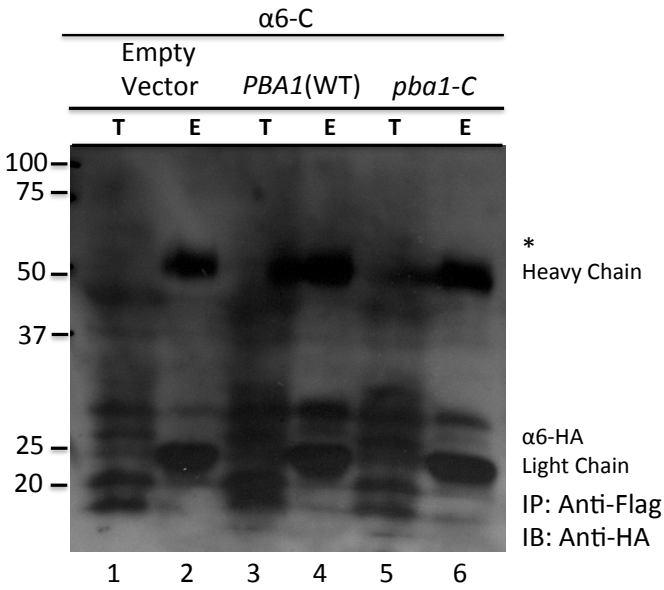

Figure 17 Pba1p-α6 BMOE Crosslinking Under Reducing Conditions + MG132 + Flag Pull-Down

Pba1p and α6 were each engineered with cysteine residues (C). These cysteines will come within close proximity of one another if the α5-α6 pocket is the correct binding site for Pba1p. Prior to crosslinking, the samples were incubated in proteasome inhibitor MG132. In all of the preceding representative blots, the method of lysis was spheroplasting, however the cells in this experiment were lysed by bead beating. Disulfide crosslinking was induced by incubating whole cell lysate from 50 ml cultures in BMOE for 60 minutes. Total fractions (20 µl) of the lysate were collected (T), and the remaining lysate was incubated in M2 Flag resin. The flag-tagged Pba1 proteins were eluted by boiling the resin in 20 µl sample buffer (E). After reducing SDS-PAGE (10%), the crosslinking was visualized by anti-HA immunoblotting. Within the Pba1p wild-type and crosslinkable eluate lanes (4 and 6) there is a band present at approximately 30 kDa corresponding to the α6-HA species. This band is not observed in the empty vector eluate lane (2). The Pba1p-α6 crosslink was expected in lane 6 at approximately 60 kDa (position denoted with an *); however, no such band was observed. Strains used were AKY689 (lanes 1 and 2), AKY690 (lane 3 and 4), AKY691 (lane 5 and 6).

REFERENCES

REFERENCES

Arrigo AP, Tanaka K, Goldberg AL, Welch WJ (1988) Identity of the 19S 'prosome' particle with the large multifunctional protease complex of mammalian cells (the proteasome). *Nature* **331:** 192-194

Breitschopf K, Bengal E, Ziv T, Admon A, Ciechanover A (1998) A novel site for ubiquitination: the N-terminal residue, and not internal lysines of MyoD, is essential for conjugation and degradation of the protein. *EMBO J* **17:** 5964-5973

Chen P, Hochstrasser M (1995) Biogenesis, structure and function of the yeast 20S proteasome. *EMBO J* **14:** 2620-2630

Dange T, Smith D, Noy T, Rommel PC, Jurzitza L, Cordero RJ, Legendre A, Finley D, Goldberg AL, Schmidt M (2011) Blm10 protein promotes proteasomal substrate turnover by an active gating mechanism. *J Biol Chem* **286:** 42830-42839

DeMartino GN, Slaughter CA (1999) The proteasome, a novel protease regulated by multiple mechanisms. *J Biol Chem* **274:** 22123-22126

Eytan E, Ganoth D, Armon T, Hershko A (1989) ATP-dependent incorporation of 20S protease into the 26S complex that degrades proteins conjugated to ubiquitin. *Proc Natl Acad Sci U S A* **86:** 7751-7755

Ghaemmaghami S, Huh WK, Bower K, Howson RW, Belle A, Dephoure N, O'Shea EK, Weissman JS (2003) Global analysis of protein expression in yeast. *Nature* **425:** 737-741

Glickman MH, Rubin DM, Coux O, Wefes I, Pfeifer G, Cjeka Z, Baumeister W, Fried VA, Finley D (1998) A subcomplex of the proteasome regulatory particle required for ubiquitin-conjugate degradation and related to the COP9-signalosome and eIF3. *Cell* **94:** 615-623

Groettrup M, Kirk CJ, Basler M (2010) Proteasomes in immune cells: more than peptide producers? *Nat Rev Immunol* **10:** 73-78

Groettrup M, Standera S, Stohwasser R, Kloetzel PM (1997) The subunits MECL-1 and LMP2 are mutually required for incorporation into the 20S proteasome. *Proc Natl Acad Sci U S A* **94:** 8970-8975

Groll M, Ditzel L, Lowe J, Stock D, Bochtler M, Bartunik HD, Huber R (1997) Structure of 20S proteasome from yeast at 2.4 A resolution. *Nature* **386:** 463-471

Heinemeyer W, Fischer M, Krimmer T, Stachon U, Wolf DH (1997) The active sites of the eukaryotic 20 S proteasome and their involvement in subunit precursor processing. *J Biol Chem* **272:** 25200-25209

Heinemeyer W, Ramos PC, Dohmen RJ (2004) The ultimate nanoscale mincer: assembly, structure and active sites of the 20S proteasome core. *Cell Mol Life Sci* **61:** 1562-1578

Hirano Y, Hayashi H, Iemura S, Hendil KB, Niwa S, Kishimoto T, Kasahara M, Natsume T, Tanaka K, Murata S (2006) Cooperation of multiple chaperones required for the assembly of mammalian 20S proteasomes. *Mol Cell* **24:** 977-984

Hirano Y, Hendil KB, Yashiroda H, Iemura S, Nagane R, Hioki Y, Natsume T, Tanaka K, Murata S (2005) A heterodimeric complex that promotes the assembly of mammalian 20S proteasomes. *Nature* **437:** 1381-1385

Hirano Y, Kaneko T, Okamoto K, Bai M, Yashiroda H, Furuyama K, Kato K, Tanaka K, Murata S (2008) Dissecting beta-ring assembly pathway of the mammalian 20S proteasome. *EMBO J* **27:** 2204-2213

Hochstrasser M (2009) Origin and function of ubiquitin-like proteins. *Nature* **458:** 422-429

Hough R, Pratt G, Rechsteiner M (1987) Purification of two high molecular weight proteases from rabbit reticulocyte lysate. *J Biol Chem* **262:** 8303-8313

Ishiura S, Sugita H (1986) Ingensin, a high-molecular-mass alkaline protease from rabbit reticulocyte. *J Biochem* **100:** 753-763

Knowlton JR, Johnston SC, Whitby FG, Realini C, Zhang Z, Rechsteiner M, Hill CP (1997) Structure of the proteasome activator REGalpha (PA28alpha). *Nature* **390:** 639-643

Kusmierczyk AR, Hochstrasser M (2008) Some assembly required: dedicated chaperones in eukaryotic proteasome biogenesis. *Biol Chem* **389:** 1143-1151

Kusmierczyk AR, Kunjappu MJ, Funakoshi M, Hochstrasser M (2008) A multimeric assembly factor controls the formation of alternative 20S proteasomes. *Nat Struct Mol Biol* **15:** 237-244

Kusmierczyk AR, Kunjappu MJ, Kim RY, Hochstrasser M (2011) A conserved 20S proteasome assembly factor requires a C-terminal HbYX motif for proteasomal precursor binding. *Nat Struct Mol Biol* **18:** 622-629

Lander GC, Estrin E, Matyskiela ME, Bashore C, Nogales E, Martin A (2012) Complete subunit architecture of the proteasome regulatory particle. *Nature* **482:** 186-191

Le Tallec B, Barrault MB, Courbeyrette R, Guerois R, Marsolier-Kergoat MC, Peyroche A (2007) 20S proteasome assembly is orchestrated by two distinct pairs of chaperones in yeast and in mammals. *Mol Cell* **27:** 660-674

Li X, Kusmierczyk AR, Wong P, Emili A, Hochstrasser M (2007) beta-Subunit appendages promote 20S proteasome assembly by overcoming an Ump1-dependent checkpoint. *EMBO J* **26:** 2339-2349

Mao I, Liu J, Li X, Luo H (2008) REGgamma, a proteasome activator and beyond? *Cell Mol Life Sci* **65:** 3971-3980

Marques AJ, Glanemann C, Ramos PC, Dohmen RJ (2007) The C-terminal extension of the beta7 subunit and activator complexes stabilize nascent 20 S proteasomes and promote their maturation. *J Biol Chem* **282:** 34869-34876

McGuire MJ, DeMartino GN (1986) Purification and characterization of a high molecular weight proteinase (macropain) from human erythrocytes. *Biochim Biophys Acta* **873:** 279-289

Murata S, Sasaki K, Kishimoto T, Niwa S, Hayashi H, Takahama Y, Tanaka K (2007) Regulation of CD8+ T cell development by thymus-specific proteasomes. *Science* **316:** 1349-1353

Park S, Kim W, Tian G, Gygi SP, Finley D (2011) Structural defects in the regulatory particle-core particle interface of the proteasome induce a novel proteasome stress response. *J Biol Chem* **286:** 36652-36666

Rabl J, Smith DM, Yu Y, Chang SC, Goldberg AL, Cheng Y (2008) Mechanism of gate opening in the 20S proteasome by the proteasomal ATPases. *Mol Cell* **30:** 360-368

Ramos PC, Hockendorff J, Johnson ES, Varshavsky A, Dohmen RJ (1998) Ump1p is required for proper maturation of the 20S proteasome and becomes its substrate upon completion of the assembly. *Cell* **92:** 489-499

Rechsteiner M, Hill CP (2005) Mobilizing the proteolytic machine: cell biological roles of proteasome activators and inhibitors. *Trends Cell Biol* **15:** 27-33

Saeki Y, Tanaka K (2012) Assembly and function of the proteasome. *Methods Mol Biol* **832:** 315-337

Schmid HP, Akhayat O, Martins De Sa C, Puvion F, Koehler K, Scherrer K (1984) The prosome: an ubiquitous morphologically distinct RNP particle associated with repressed mRNPs and containing specific ScRNA and a characteristic set of proteins. *EMBO J* **3:** 29-34

Schmidt F, Dahlmann B, Hustoft HK, Koehler CJ, Strozynski M, Kloss A, Zimny-Arndt U, Jungblut PR, Thiede B (2011) Quantitative proteome analysis of the 20S proteasome of apoptotic Jurkat T cells. *Amino Acids* **41:** 351-361

Scott CM, Kruse KB, Schmidt BZ, Perlmutter DH, McCracken AA, Brodsky JL (2007) ADD66, a gene involved in the endoplasmic reticulum-associated degradation of alpha-1-antitrypsin-Z in yeast, facilitates proteasome activity and assembly. *Mol Biol Cell* **18:** 3776-3787

Smith DM, Chang SC, Park S, Finley D, Cheng Y, Goldberg AL (2007) Docking of the proteasomal ATPases' carboxyl termini in the 20S proteasome's alpha ring opens the gate for substrate entry. *Mol Cell* **27:** 731-744

Tamura T, Nagy I, Lupas A, Lottspeich F, Cejka Z, Schoofs G, Tanaka K, De Mot R, Baumeister W (1995) The first characterization of a eubacterial proteasome: the 20S complex of Rhodococcus. *Curr Biol* **5:** 766-774

Tanaka K (1994) Role of proteasomes modified by interferon-gamma in antigen processing. *J Leukoc Biol* **56:** 571-575

Tian G, Park S, Lee MJ, Huck B, McAllister F, Hill CP, Gygi SP, Finley D (2011) An asymmetric interface between the regulatory and core particles of the proteasome. *Nat Struct Mol Biol* **18:** 1259-1267

Ustrell V, Hoffman L, Pratt G, Rechsteiner M (2002) PA200, a nuclear proteasome activator involved in DNA repair. *EMBO J* **21:** 3516-3525

van Nocker S, Vierstra RD (1993) Multiubiquitin chains linked through lysine 48 are abundant in vivo and are competent intermediates in the ubiquitin proteolytic pathway. *J Biol Chem* **268:** 24766-24773

Velichutina I, Connerly PL, Arendt CS, Li X, Hochstrasser M (2004) Plasticity in eucaryotic 20S proteasome ring assembly revealed by a subunit deletion in yeast. *EMBO J* **23:** 500-510

Volker C, Lupas AN (2002) Molecular evolution of proteasomes. *Curr Top Microbiol Immunol* **268:** 1-22

Welchman RL, Gordon C, Mayer RJ (2005) Ubiquitin and ubiquitin-like proteins as multifunctional signals. *Nat Rev Mol Cell Biol* **6:** 599-609

Wilk S, Orlowski M (1983) Evidence that pituitary cation-sensitive neutral endopeptidase is a multicatalytic protease complex. *J Neurochem* **40:** 842-849

Wolf S, Nagy I, Lupas A, Pfeifer G, Cejka Z, Muller SA, Engel A, De Mot R, Baumeister W (1998) Characterization of ARC, a divergent member of the AAA ATPase family from Rhodococcus erythropolis. *J Mol Biol* **277:** 13-25

Xie Y, Varshavsky A (2001) RPN4 is a ligand, substrate, and transcriptional regulator of the 26S proteasome: a negative feedback circuit. *Proc Natl Acad Sci U S A* **98:** 3056-3061

Xu P, Duong DM, Seyfried NT, Cheng D, Xie Y, Robert J, Rush J, Hochstrasser M, Finley D, Peng J (2009) Quantitative proteomics reveals the function of unconventional ubiquitin chains in proteasomal degradation. *Cell* **137:** 133-145

Yashiroda H, Mizushima T, Okamoto K, Kameyama T, Hayashi H, Kishimoto T, Niwa S, Kasahara M, Kurimoto E, Sakata E, Takagi K, Suzuki A, Hirano Y, Murata S, Kato K, Yamane T, Tanaka K (2008) Crystal structure of a chaperone complex that contributes to the assembly of yeast 20S proteasomes. *Nat Struct Mol Biol* **15:** 228-236

Zhang X, Stoffels K, Wurzbacher S, Schoofs G, Pfeifer G, Banerjee T, Parret AH, Baumeister W, De Mot R, Zwickl P (2004) The N-terminal coiled coil of the Rhodococcus erythropolis ARC AAA ATPase is neither necessary for oligomerization nor nucleotide hydrolysis. *J Struct Biol* **146:** 155-165

Zhang Z, Clawson A, Realini C, Jensen CC, Knowlton JR, Hill CP, Rechsteiner M (1998) Identification of an activation region in the proteasome activator REGalpha. *Proc Natl Acad Sci U S A* **95:** 2807-2811

Zhong L, Belote JM (2007) The testis-specific proteasome subunit Prosalpha6T of D. melanogaster is required for individualization and nuclear maturation during spermatogenesis. *Development* **134:** 3517-3525

Zuhl F, Seemuller E, Golbik R, Baumeister W (1997) Dissecting the assembly pathway of the 20S proteasome. *FEBS Lett* **418:** 189-194

Zwickl P, Kleinz J, Baumeister W (1994) Critical elements in proteasome assembly. *Nat Struct Biol* **1:** 765-770

Zwickl P, Ng D, Woo KM, Klenk HP, Goldberg AL (1999) An archaebacterial ATPase, homologous to ATPases in the eukaryotic 26 S proteasome, activates protein breakdown by 20 S proteasomes. *J Biol Chem* **274:** 26008-26014